UC Davis

UC Davis Electronic Theses and Dissertations

Title

The Effects of Short- and Long-Chain PFAS On In Vitro Triple Negative Breast Cancer Progression

Permalink

https://escholarship.org/uc/item/28j093fg

Author

Delgadillo, Hector Antonio

Publication Date

2024

Peer reviewed|Thesis/dissertation

eScholarship.org Powered by the California Digital Library
University of California

The Effects of Short- and Long-Chain PFAS On *In Vitro* Triple Negative Breast Cancer Progression

By

HECTOR ANTONIO DELGADILLO

THESIS

Submitted in partial satisfaction of the requirements for the degree of

MASTER OF SCIENCE

in

Pharmacology and Toxicology

in the

OFFICE OF GRADUATE STUDIES

of the

UNIVERSITY OF CALIFORNIA

DAVIS

Approved:

_____

Michele A. La Merrill, Chair

_____

Allison K. Ehrlich

_____

John D. Furlow

Committee in Charge

2024

The Effects of Short- and Long-Chain PFAS On *In Vitro* Triple Negative Breast Cancer Progression

Hector A. Delgadillo

University of California, Davis

2024

ABSTRACT

Per- and polyfluoroalkyl substances (PFAS) are a class of compounds commonly used as surfactants in food contact materials and household items due to their hydrophobicity. However, their physicochemical properties render them highly resistant to degradation in the environment and human body. Thus, these chemicals are environmentally ubiquitous and have been found in the serum of 98% of U.S. citizens. Evidence implicates some well characterized PFAS in breast cell carcinogenesis and cancer progression. While PFAS-induced receptor-positive breast cancer progression has been widely investigated, PFAS-induced receptor-negative breast cancer has not, and molecular mechanisms remain unclear. Additionally, Generalized Read-Across of PFAS using cancer progression endpoints are lacking. This research analyzes and compares the effects of five PFAS of increasing alkyl chain length on triple negative breast cancer progression *in vitro*. Using the aggressive human cell line Hs578T the effects of five PFAS were analyzed across environmentally relevant concentrations. Progression was assessed through 2D cell proliferation assays and “2.5D” Matrigel migration and invasion assays. Results showed significant decreases in mean number of protrusions per cell and total colony formation per well with PFBA and PFDoA treatment. Significant decreases in colony formation were

observed with PFDA treatment at all concentrations. The mean length of the longest protrusion per cell was largely unimpacted by PFAS, except for decreases by PFDoA. When viewing the data though read-across lenses, near significant trends were seen in protrusion counts with increasing alkyl chain length at 1 nM and 10 nM PFAS. The highest alkyl length significantly decreased colony formation in a pattern seen across 10 nM, 100 nM and 1000 nM concentrations. Cell proliferation was not impacted by PFAS treatment. These results will help elucidate whether triple negative breast cancer progression is related to concentrations and alkyl chain length, and whether short-chain PFAS exhibit increased progression as longer PFAS have been shown to promote.

Table of contents

Introduction 1

Materials and Methods 6

Cell Culture 6

PFAS selection 7

PFAS concentrations 8

2.5D Cell Invasion Assay (“3D On-Top”) 9

2D Cell Proliferation Assay 12

Statistical Analysis 13

Results 14

Concentration effects on invasive protrusion formation in Hs578T cells 15

Concentration effects on total colony formation per well in Hs578T cells 17

Alkyl chain length effects on invasive protrusion formation in Hs578T cells 18

Alkyl chain length effects on total colony formation per well in Hs578T cells 20

Concentration effects on mean live and dead cell number per well 22

Alkyl chain length effects on mean live cell number per well 24

Discussion 26

Future Work 32

Conclusions 35

References 36

Table 1: Abbreviation References

Acronym	Complete Term
PFAS	Per- and polyfluoroalkyl substances
PFBA	Perfluorobutanoic acid
PFHxA	Perfluorohexanoic acid
PFHpA	Perfluoroheptanoic acid
PFOA	Perfluorooctanoic acid
PFOS	Perfluorooctane sulfonic acid
PFNA	Perfluorononanoic acid
PFDA	Perfluorodecanoic acid
PFDoA	Perfluorododecanoic acid
U.S.	United States
U.S. EPA	United States Environmental Protection Agency
GenRA	Generalized Read-Across
IARC	International Agency for Research on Cancer
NHANES	National Health and Nutrition Examination Survey
TNBC	Triple negative breast cancer
DMSO	Dimethyl sulfoxide
FBS	Fetal bovine serum
SF	Serum free (no FBS)
NF-κB	Nuclear factor kappa B
PPARα/γ	Peroxisome proliferator-activated receptor-alpha and -gamma
HER2	Human epidermal growth factor receptor 2
Hs578T	Human triple negative breast cancer cell line
MCF10A	Human receptor-negative breast epithelial cell line
MDA-MB-231	Human triple negative breast cancer cell line
qPCR	Quantitative polymerase chain reaction
EdU	5-ethynyl-2'-deoxyuridine (cell proliferation assay)
SEM	Standard error mean

Introduction

Per- and polyfluoroalkyl substances (PFAS) are a class of highly fluorinated chemicals that vary in their alkyl chain lengths and functional groups. They are commonly incorporated as surfactants in everyday products such as food packaging materials, nonstick cookware, upholstery, and personal care products due to their excellent oil and water repelling abilities[1, 18]. These abilities are a result of the incredibly strong carbon-fluorine bonds which give the class of chemicals their renowned fluorinated characteristic. However, due to these bonds, they have become ubiquitous, persistent environmental contaminants presently detected in resources such as drinking water[8], aquatic and animal-derived food[2, 60, 66] and indoor dust[52], the latter two being found in markedly high concentrations. For example, Barbo et al, 2023[2] sampled freshwater fish across >500 sites in the United States (U.S.) for PFAS compound quantification. The researchers found perfluorooctane sulfonic acid (PFOS) concentrations to be 2400x higher than the United States Environmental Protection Agency's (U.S. EPA) Lifetime Health Advisory Limit of 0.02 parts per thousand (ppt). This is equivalent to one month of water consumption at 48 ppt PFOS and demonstrates their environmental presence. Due to their environmental presence, PFAS are ingested or inhaled by humans and have been detected in the serum of 98% of individuals sampled by the National Health and Nutrition Examination Survey[11] (NHANES). Further, PFAS can sequester within the human body for upwards of three decades for some long-chain PFAS, specifically in the kidneys, liver, and blood proteins[58]. These chemicals also display bioaccumulation and biomagnification abilities in non-human mammals[6], further highlighting their propensity to sequester in tissues. Currently, it is estimated that nearly 15,000 PFAS exist[40] and 600 PFAS are currently used in industry[21], but only six are regulated in drinking water by the U.S. EPA[41]

and few have been well characterized by their health effects. Additionally, long-chain PFAS are being replaced by short-chain alternatives in industry[35] as data on long-chain PFAS toxicity emerges. The effects of a couple of long-chain PFAS commonly found in human serum have been described previously. Perfluorooctanoic acid (PFOA) and PFOS are two highly studied long-chain PFAS with great evidence linking them to numerous illnesses, such as high cholesterol, thyroid disease, and cancers[16, 37, 68]. Additionally, a large body of *in vitro*, *in vivo*, and epidemiological evidence supports the carcinogenicity of these two PFAS[7, 33, 44, 46, 47, 51, 57], leading to their classifications as a Group 1 Carcinogen to Humans for PFOA and Group 2B Possible Carcinogen to Humans for PFOS by the International Agency for Research on Cancer (IARC)[67]. However, the link between carcinogenesis or cancer progression and the many other PFAS currently detected in human serum is unclear, sometimes with contrasting results. For example, the 2021 Toxicological Profile for Perfluoroalkyls[58] released by the U.S. Department of Health and Human Services (DHHS) states there are no consistent associations between breast cancer risk and three long-chain PFAS. Yang et al., 2024[65] conducted a dose-response meta-analysis including 748,188 participants to identify whether long-chain PFAS serum exposure significantly increase the odds of cancer incidence. These researchers found similar results to the DHHS. In contrast, Velarde et al., 2022[61] found significant associations between long-chain PFAS and breast cancer incidence in Filipina women from industrialized regions of the Philippines. Meanwhile, significant data absences exist for short-chain alternatives given their recency of substitution for long-chain PFAS, but current epidemiological data show no cancer effects of these chemicals[58].

Breast cancer is the second most common cancer in women and leading cause of cancer related deaths in women of Hispanic and African American ancestry[9]. Triple negative breast cancers (TNBCs) are a cancer subtype comprising 10 - 15% of breast cancer cases and are characterized by their lack of three cell surface proteins (progesterone receptor, estrogen receptor, human epidermal growth factor receptor 2 (HER2)) which are common pharmacological targets. Thus, TNBC substantially lacks therapeutic options and is the most aggressive breast cancer type with the highest metastasis likelihood and lowest breast cancer 5-year survival rate[55] of 77%. Disparities in TNBC are well documented, with Black women experiencing significantly higher incidence rates than all other races[19]. Further, incidence rates are increasing in some populations[19].

Studies on chemical exposure disparities among demographic groups are seldom but increasingly generated to aid in the understanding of how these chemicals may affect certain populations differently than others. Nelson et al., 2012[34] found perfluorononanoic acid (PFNA) to be highest in non-Hispanic Black individuals. Specifically looking at women, Nguyen et al., 2020[36] found perfluorodecanoic acid (PFDA) to be highest in non-Hispanic Black women and other races. Similarly, Calafat et al., 2007[12] found PFOS and PFNA to be significantly higher in non-Hispanic Black individuals greater than 55 years of age relative to non-Hispanic white individuals. These three studies utilized publicly available NHANES datasets, but some researchers also focus on smaller communities within the U.S. For example, Liu et al., 2022[32] investigated two populations in Western New York state, Anglers and Burmese refugees, who consume PFAS contaminated freshwater fish at differing rates. This study found that anglers were mostly well-educated

non-Hispanic whites who were highly aware of fish advisories. In contrast, most Burmese refugees had no more than four years of education, were of low socioeconomic status, and were not aware of fish advisories thus consuming 5.5x more fish. Consequently, they displayed 3x higher serum PFOS levels than anglers and 8x greater than NHANES sampled individuals. These four examples demonstrate that PFAS disparities exist in the general U.S. population and within smaller, more specific U.S. communities. Reasons why exposure disparities may exist among demographic groups include culturally and personally related consumer choices, household income, food security, education, and occupation[34] to name a few.

As aforementioned, TNBC and PFAS disparities exist within the U.S population and can overlap such as in black women. Some long-chain PFAS are present at higher levels in individuals who are more susceptible to TNBC. However, studies investigating PFAS-driven TNBC progression are severely lacking. PFAS interference of canonical progesterone, estrogen, and HER2 signaling has been demonstrated to occur *in vitro* and *in vivo*[29, 33, 64], leading to well-evidenced hypotheses on mechanistic drivers of receptor-positive breast cancers. In contrast, mechanisms have not been concretely identified in TNBC. Wang et al, 2024[63] aimed to elucidate these mechanisms using 3D TNBC cell models, finding that the PFOA-induced Hippo pathway drives epithelial-to-mesenchymal characteristics and invasive phenotypes. Zhang et al., 2014[69] found PFOA-driven nuclear factor kappa B (NF-κB) signaling in TNBC cell invasion, and Sakai et al., 2022[50] implicates the peroxisome proliferator-activated receptor-alpha (PPARα) as a driver of migration after PFOA treatment. These are the only three studies we are aware of that investigate the PFAS – TNBC relationship.

Data gaps exist for both short- and long-chain PFAS. Generalized Read-Across (GenRA) is a method commonly employed by risk assessors such as the U.S. EPA to resolve data gaps on a chemical's biological effects, wherein researchers use available data from well-characterized chemicals to predict endpoints for similar, data-poor chemicals[22]. For example, reported data outcomes from *in vitro* toxicity assays following perfluoroheptanoic acid (PFHpA) treatment may be used to predict outcomes for the structurally similar perfluorohexanoic acid (PFHxA) using a GenRA approach, as is described in Shah et al., 2016[53]. In this paper, 50 toxicity endpoints from developmental, multigenerational, and sub chronic studies following PFAS treatment are assessed. 9 PFAS are subsequently mapped and compared to PFHxA by chemical and bioactivity fingerprints. However, it is unclear if this method can be applied in terms of toxicity outcomes related to cancer progression.

To this end, this study investigated short- and long-chain PFAS effects *on in vitro* TNBC cell proliferation, migration, and invasion across an environmentally relevant concentration gradient and aimed to elucidate the molecular mechanisms involved in the cancer progression. This study investigated the concentration-dependent responses of PFAS commonly found in human serum. It also investigated the alkyl chain effects to better understand whether long-chain PFAS promote greater breast cancer progression than short-chain alternatives. Concurrently, short- and long-chain PFAS data will be compared amongst each other to assess whether similar outcomes are found, thus revealing whether GenRA approaches may be applied in cancer progression bioassays involving phenotypic and molecular data.

Materials and Methods

Cell culture

TNBC cell line Hs578T was obtained from the American Type Culture Collection (Manassas, VA). The cells were cultured in T75 flasks (Cat. FB012937) in complete growth medium containing Gibco Dulbecco's Modified Eagle's Medium (Cat. 11960-044), 1% Gibco Penicillin-Streptomycin (Cat. 15140122), 1% Gibco Sodium Pyruvate (Cat. 11360070), 2% Gibco GlutaMAX Supplement (Cat. 35050061) (all Thermo Fisher Scientific; Waltham, MA), 10% fetal bovine serum (Cat. 100-106, GeminiBio; Sacramento, CA), and 0.1% Gibco recombinant human insulin (Cat. Z101065, ABM; Richmond, BC, CAN) dissolved in 0.1 N hydrochloric acid (Cat. Cat. L-11775, Thermo Fisher Scientific; Waltham, MA). Cells were incubated at 37 °C and 5% CO_2 until reaching 90% confluence before passage using 0.25% trypsin (Cat. 25200056, Thermo Fisher Scientific; Waltham, MA). The cell line was selected due to its thorough characterization in the literature and our previous research indicating the cells to be affected by PFAS treatment.

PFAS Selection

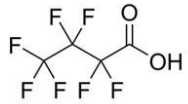
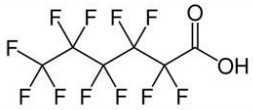
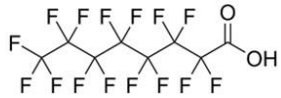
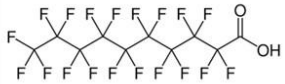
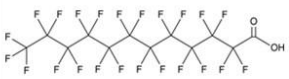
PFAS name	PFAS acronym	DTXSID	Carbon length	Chemical structure	Half-life	Mean Biomonitoring CA Geometric Mean (nM)
Perfluorobutanoic Acid	PFBA	4059916	4		72 – 81 hours	0.3
Perfluorohexanoic Acid	PFHxA	3031862	6		14 – 49 days	0.58
Perfluorooctanoic Acid	PFOA	8031865	8		2.1 – 10.1 years	3.78
Perfluorodecanoic Acid	PFDA	3031860	10		> 4 years	0.63
Perfluorododecanoic Acid	PFDoA	8031861	12		Unknown	0.03

Table 2: Comparison of properties among the five PFAS chosen for the *in vitro* study. The table contains the PFAS full name, commonly used acronym, DTXSID, alkyl chain length, chemical structure, estimated human serum half-life, and mean Geometric Mean of all Biomonitoring California studies detecting the PFAS in human serum. Note: PFDoA was detected in only one of these studies, hence it is not a mean of geometric means but a single value.

Five structurally similar PFAS of varying alkyl chain lengths were selected to analyze concentration- and alkyl chain length-dependent outcomes. These five PFAS are designated as priority chemicals[13] currently detected in human serum from cross-state general California population sampling conducted by Biomonitoring California, a program run by the California Department of Public Health and California Environmental Protection Agency. These PFAS include perfluorobutanoic acid (PFBA) (98% purity, Cat.164194, Millipore Sigma; Milwaukee, WI), perfluorohexanoic acid (PFHxA) (95% purity, Cat. 307-24-4, AAblocks; San Diego, CA), perfluorooctanoic acid (PFOA) (96% purity, Cat. AC173960250, Acros Organics; Geel, AN, BE), perfluorodecanoic acid (PFDA) (98%

purity, Cat. 177741, Sigma-Aldrich; St. Louis, MO), and perfluorododecanoic acid (PFDoA) (96% purity, Cat. L14113, Alfa Aesar; Ward Hill, MA). Short-chain PFAS include PFBA and PFHxA while long-chain PFAS include PFOA, PFDA, and PFDoA. All PFAS were extensively vortexed into 10 mM master stocks in ≥99.9% pure dimethyl sulfoxide (DMSO) (Cat. 472301, Sigma-Aldrich; St. Louis, MO) until visibly dissolved.

PFAS Concentrations

PFAS treatment concentrations for *in vitro* assays were informed by literature (2009 – 2024) describing PFAS concentrations in food and water resources and in human serum. A deep literature mining project was employed to collect all currently existing data from publicly available state and federal databases, technical reports, and publications available online. Initially, the project focused on PFDoA and concentrations were informed by this chemical's environmental levels. Subsequent literature mining found the additional four chemicals to have comparable concentrations in human serum and resources[5, 8, 28, 32, 38, 42, 48, 52, 56, 59, 60, 61, 66]. Four PFAS concentrations were ultimately chosen: 1 nM, 10 nM, 100 nM, and 1000 nM. 0 - 10 nM concentrations are found in human serum while 10 – 1000 nM are found in food sources and indoor dust. Working stocks of 1 µM, 10 µM, 100 µM, and 1000 µM PFAS were prepared in ≥99.9% pure DMSO from well-vortexed 10 mM master stocks.

2.5D Cell Invasion Assay ("3D On-Top")

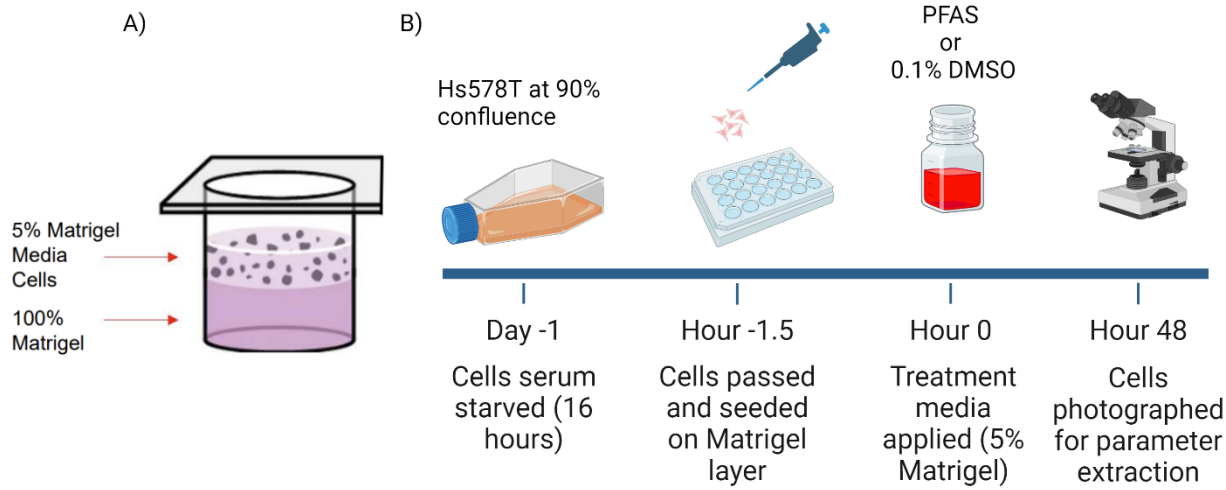


Figure 1: Human breast cancer cell line Hs578T 2.5D cell invasion assay. A) Schematic demonstrating the 2.5D invasion assay. Cells were seeded on a Matrigel layer and allowed to adhere prior to PFAS or control treatment. After 48 hours, cells were imaged at 4x and 20x magnification for parameter extraction. B) Timeline of experimental procedures.

Since the discovery of cell culture in 1885, the scientific feat of growing cells in monolayers in the 2D environment has led to significant discoveries in the fields of biochemical, molecular, physiological, and biological sciences[43]. However, as technology advances, new methods of cell culture arise that are more representative of the human biological experience. One example is the 3D culturing of cells, spheroids, and organoids which has significantly advanced in the past decade and captures phenotypes more comparable to *in vivo* models[20]. Cell phenotype and gene expression has been previously shown to significantly differ in 2D versus 3D cell culture[27]. Thus, we grew cells on growth factor reduced Matrigel (Cat. 354230, Corning; Tewksbury, MA) which is rich in laminin, collagen IV, and heparan, among other structural proteins, and mimics the basement membrane of human tissues[23]. Hs578T cells were seeded on a layer of polymerized Matrigel in 5% fetal bovine serum (FBS) culture media with PFAS treatment or 0.1%

DMSO control, informed by the protocol described by Lee et al., 2010[30]. Given the method of seeding individual cells on top (rather than spheroids within) of Matrigel, the assay is coined as the 2.5D assay. Matrigel aliquots were stored at -20 °C long-term and thawed the night before the assay was performed in a container of ice at 4 °C. Matrigel was not thawed more than twice before use. Hs578T cells were serum-starved in T75 flasks for 16 hours prior to the assay to synchronize the cells' replication cycles. Optimization experiments were employed, revealing 200 µL Matrigel and 8,000 cells per well in 24-well plates were ideal for the 2.5D assay. Wells were rinsed with serum free media for proper Matrigel dispersion prior to coating using 200 µL liquid Matrigel. Matrigel was polymerized for 30 minutes at 37 °C followed by the addition of 8,000 cells per well in 250 µL serum free media. Cells were allowed to adhere to the Matrigel in 37 °C and 5% CO_2 for 1.5 hours to prevent potential confounding by FBS or PFAS treatment. Cells were then applied 250 µL treatment media containing 10% Matrigel and 10% FBS with or without 2, 20, 200, and 2000 nM PFAS, for a final volume of 500 µL and final concentrations of 5% Matrigel, 5% FBS, and the concentrations aforementioned. To allow the cells to reorganize their microenvironment, 5% Matrigel was included in the cell culture media, while 5% FBS media was used based on our previous cell proliferation findings indicating standard 10% FBS may abrogate PFAS-induced cell proliferation observed at lower FBS concentrations. Both procedures have been successfully used previously[27, 30]. Serum free (SF) conditions acted as a negative control as is standard in the literature across cell lines.

The cells were grown for 48 hours before imaging at 4x and 20x magnification using an Olympus CK53 inverted microscope (Evident; Tokyo, JPN) mounted with an

industrial digital camera (E3ISPM09000KPA, ToupTek; Hangzhou, ZJ, CN) compatible with the ToupView software (ToupTek; Hangzhou, ZJ, CN). Colony formation is commonly interpreted as a parameter of TNBC invasion and tumorigenesis[10, 17, 49]. Other papers have found colony formation to be indicative of cell migration given the cells' ability to move towards each other across the well to form colonies[39]. Therefore, total colony formation per well may capture both migration and invasion parameters and was used as an indicator of migration in this study. The presence of pseudopodia, also known as protrusions, has also been previously described as an indicator of a more invasive TNBC cell phenotype[15, 27, 31, 62,] thus we quantified differences in the mean number of protrusions per cell and in the length of the longest protrusion per cell in 6 individual cancer cells per treatment group per biological replicate (i.e., cell passage). The independent experiments were repeated five times with five different biological replicates. Given the sensitivity of the matrix, some wells' Matrigel coating became dislodged after media addition, possibly compromising the well's integrity for the assay. Hence, some wells did not have data obtained from them and some treatment groups are noticeably missing a biological replicate. Nevertheless, all treatment groups have at least 3 biological replicates.

At 4x, enough images were taken to capture the total colony formation per treatment group in each well across the five biological replicates. At 20x, six cells (i.e., technical replicates) per treatment group in each well across the five biological replicates were photographed for protrusion parameters. The value of six cells per treatment group was chosen for analysis after previous SAS power analyses found this value to be sufficient in detecting significant differences in protrusion counts between the negative and positive controls ($p = 0.05$). To avoid cell selection bias, the photographer closed their

eyes and shifted the well to a random field of view before focusing the microscope onto a group of cells. No more than 4 cells per field of view were analyzed. 4x colony images were blinded and data automatically extracted for colonies ≥8000 μm^2 using the Cell Colony Edge detection macros on ImageJ (https://sourceforge.net/projects/cell-colony-edge/files/). The area of 8000 μm^2 was appropriate for discerning colonies from small clusters of few elongated cells during the optimization of the 2.5D assay. 20x cell images were blinded and distributed to four researchers wherein protrusion data were manually extracted using the ImageJ measurement tools (https://imagej.net/ij/).

2D Cell Proliferation Assay

Hs578T cells were serum-starved overnight in T75 flasks for 16 hours prior to the assay to synchronize the cells' replication cycles. Cells were then passed and seeded in serum-free media in 6-well plates (Cat. FB012927, Thermo Fisher Scientific; Waltham, MA) at 10^5 cells per well. After a 1.5-hour attachment period, serum-free media was replaced with 0.1% DMSO control or treatment media (1 nM and 10 nM PFAS). These two concentrations were chosen based on results from the previous 2.5D invasion assay (see Results → PFAS effects on mean live cell number per well). Cells were allowed to proliferate for 48 hours and then trypsinized and stained by unfiltered Gibco 0.4% Trypan Blue (Cat. 15250-061, Life Technologies Corporation; Carlsbad, CA) for hemocytometer counting. Two technical replicates were sampled per well for each biological replicate, and three biological replicates were analyzed for most groups. 10 nM PFBA, 1 nM PFHxA, and 10 nM PFHxA underwent technical error thus having 2 biological replicates.

Statistical Analysis

Cell colonies and protrusions were analyzed in linear regression accounting for repeated measures within biological replicates as mixed random and fixed effects (SAS 9.0, PROC MIXED). Longest protrusions per cell were evaluated in linear regression adjusted for blinded imager and accounting for repeated measures within biological replicates as mixed random and fixed effects (SAS 9.0, PROC MIXED). Protrusion counts were evaluated in Poisson regression adjusted for blinded imager and accounting for repeated measures within biological replicates as mixed random and fixed effects (SAS 9.0, PROC GENMOD). Cell proliferation data were analyzed by One-way ANOVA with Tukey's post-hoc tests ($p = 0.05$) and simple linear regressions ($p = 0.05$) using GraphPad Prism10.1.2. All data was plotted using GraphPad Prism 10.1.2 and are reported as mean ± standard error mean (SEM).

Results

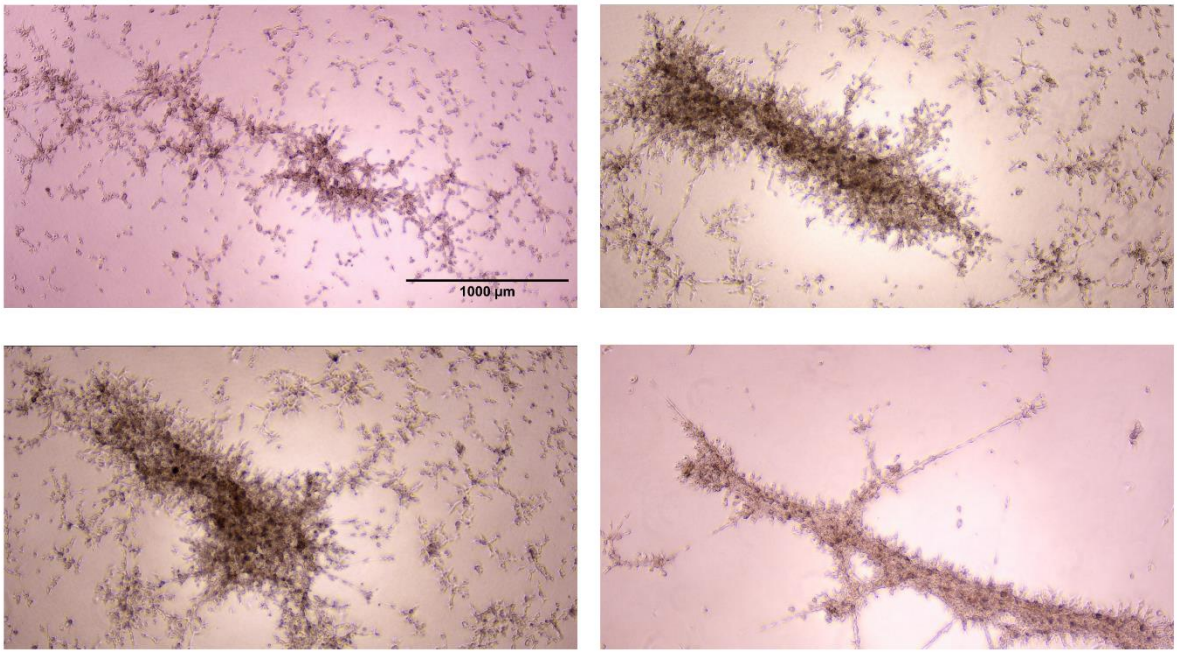


Figure 2: **Representative 4x images of colony formation after 48 hours of treatment**. Difference in media phenol red coloration is hypothesized to be caused by PFAS treatment effects on cell processes (e.g., respiration, metabolism), where more yellow coloration = pH < 7.

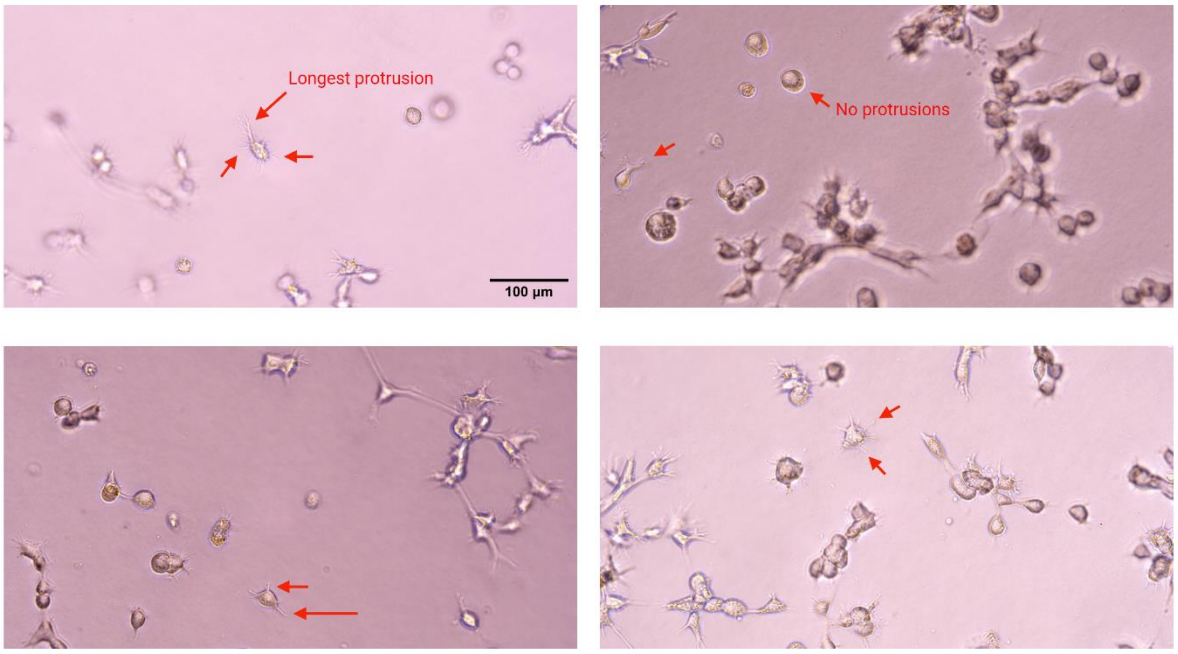


Figure 3: **Representative 20x images of individual cells with protrusions to be measured after 48 hours of treatment**. Networks connecting cells can be seen but are not analyzed in this study. Only individual cells are analyzed.

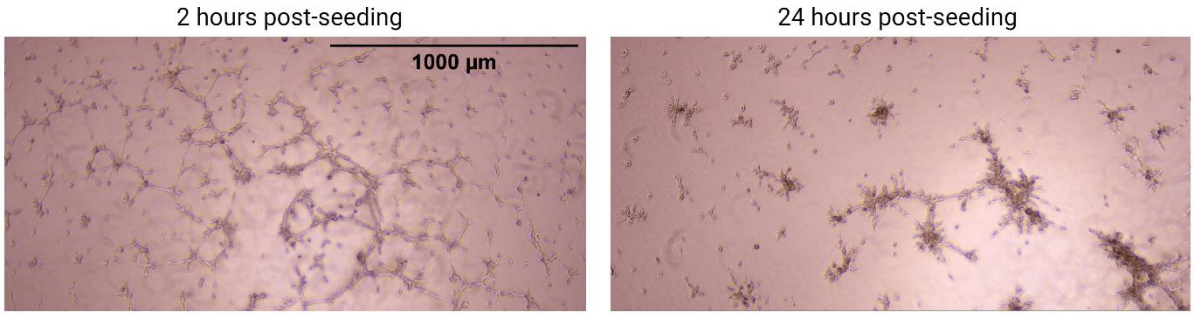


Figure 4: Representative 4x images of cell migration leading to colony formation. Cells were imaged at two- and 24-hours post-seeding. At two hours post-seeding, cells are evenly distributed across the well and begin to form networks with each other. At 24 hours post-seeding, cells migrated towards each other to form colonies.

Concentration effects on invasive protrusion formation in Hs578T cells

Across the five PFAS tested, significant concentration-dependent decreases in mean number of invasive protrusions per cell were seen in PFBA treatments of 100 nM ($p = 0.01$) and 1000 nM ($p = 0.05$), and a marginally significant decreasing trend in this group was evident (Figure 5A, $p_{trend} = 0.05$). Further, for PFDA treated groups, 1 nM ($p = 0.05$), 10 nM ($p < 0.0001$), 100 nM ($p = 0.001$), and 1000 nM ($p < 0.0001$) concentrations significantly decreased protrusion counts (Figure 5D). In PFDoA treated groups, 10 nM ($p = 0.06$) and 100 nM ($p = 0.003$) concentrations decreased protrusion counts (Figure 5E). Regarding the mean longest protrusion length per cell (Figure 6), no significant differences or significant trends were observed for most groups. However, PFDoA exhibited a significant decreasing trend ($p_{trend} = 0.02$) and 1000 nM concentration decreased the mean length longest protrusion length (Figure 6E, $p = 0.07$).

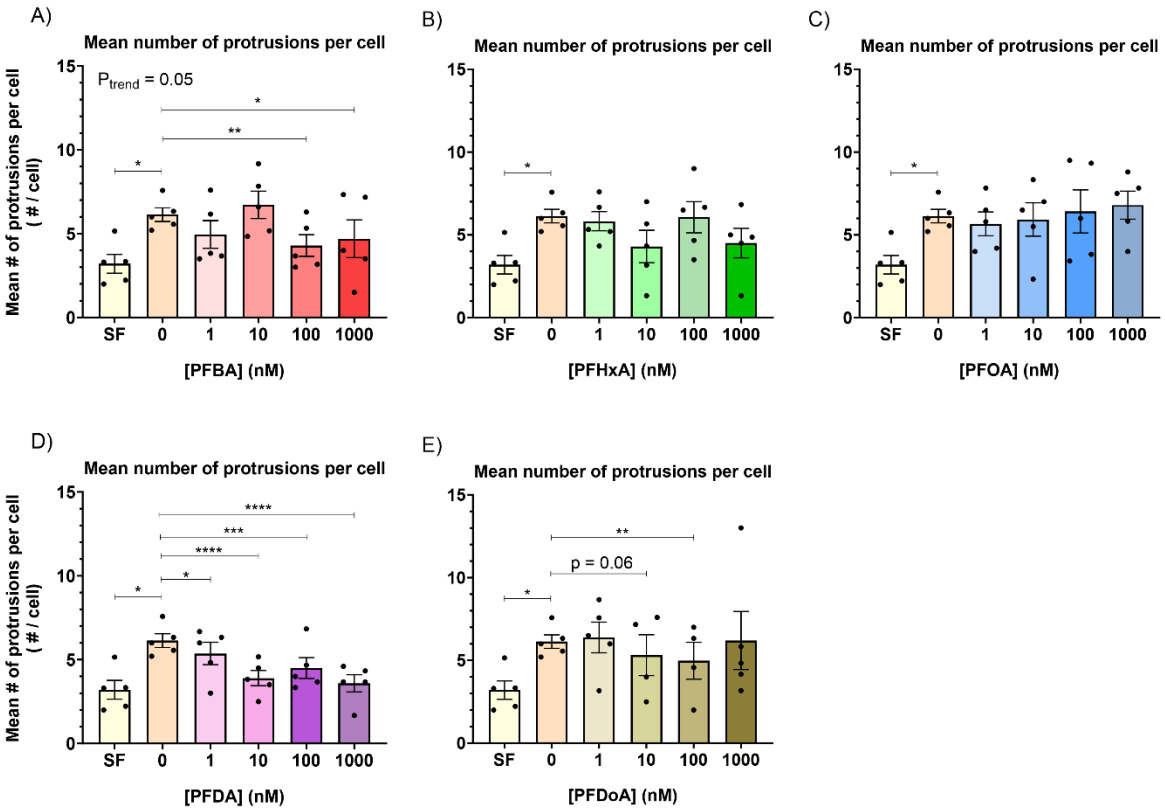


Figure 5: **Short- and long-chain PFAS concentration-response effect on Hs578T mean number of protrusions per cell**. Cell protrusion counts were measured after 48 hours of treatment of varying concentrations of A) PFBA, B) PFHxA, C) PFOA, D) PFDA, and E) PFDoA. 6 cells were measured per treatment; 5 biological replicates were run in total for most treatment groups. Significant or near significant decreases were seen in A) 100 nM and 1000 nM, D) 1 nM, 10 nM, 100 nM, and 1000 nM, and E) 10 nM and 100 nM. Decreasing trends were seen in PFBA treated groups. Figure depicts mean ± SEM. *p ≤ 0.05, **p ≤ 0.01, ***p ≤ 0.001, ****p ≤ 0.0001.

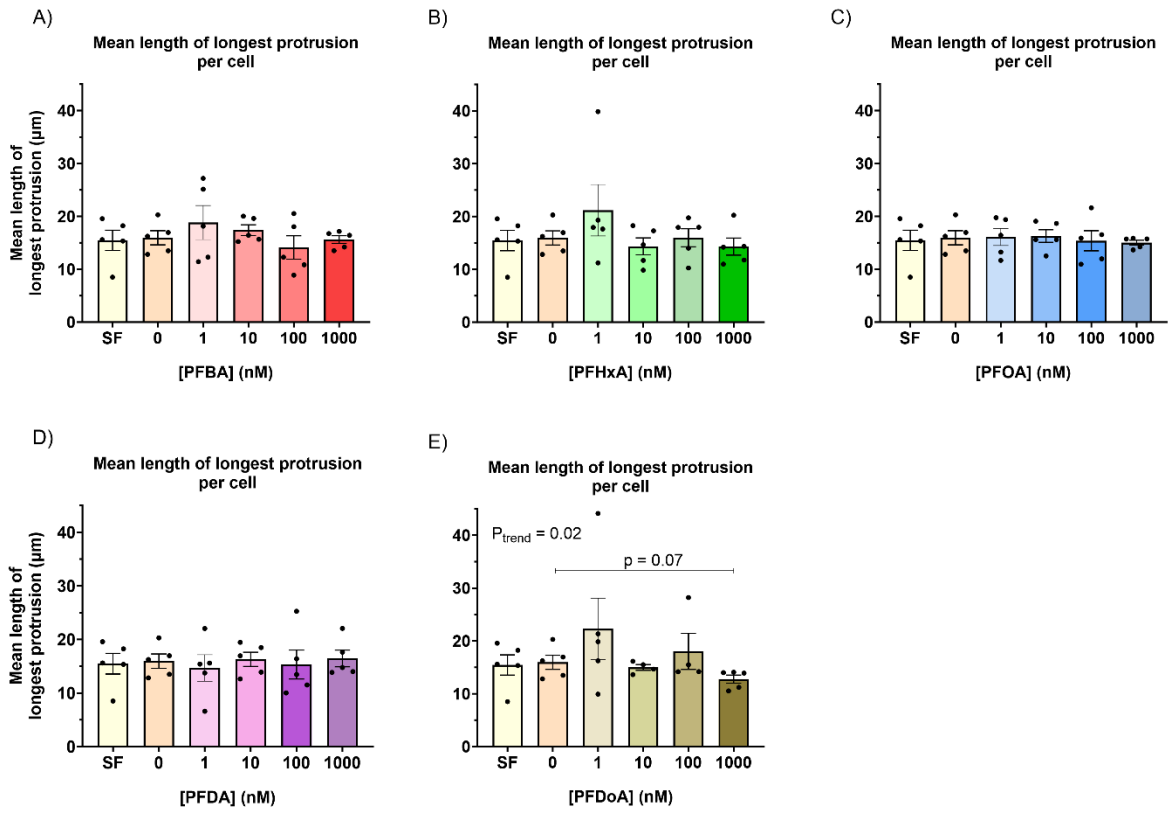


Figure 6: **Short- and long-chain PFAS concentration-response effect on Hs578T mean length of the longest protrusion per cell**. Cell protrusion lengths were measured after 48 hours of treatment of varying concentrations of A) PFBA, B) PFHxA, C) PFOA, D) PFDA, and E) PFDoA. 3 - 7 cells were measured per treatment; 5 biological replicates were run in total for most treatment groups. 1000 nM PFDoA decreased the mean longest protrusion length and PFDoA treatment exhibited a significant decreasing trend. Figure depicts mean ± SEM.

Concentration effects on total colony formation per well in Hs578T cells

Across the five PFAS tested on total colony formation per well, significant decreases were seen in 1000 nM PFBA (Figure 7A, $p = 0.009$) and a significant decreasing trend was evident in this group ($p_{trend} = 0.02$). Significant decreases were also seen in 10 nM ($p = 0.01$), 100 nM ($p = 0.05$), and 1000 nM ($p = 0.006$) PFDoA treated groups (Figure 7E) and a non-significant decreasing trend was evident ($p_{trend} = 0.07$).

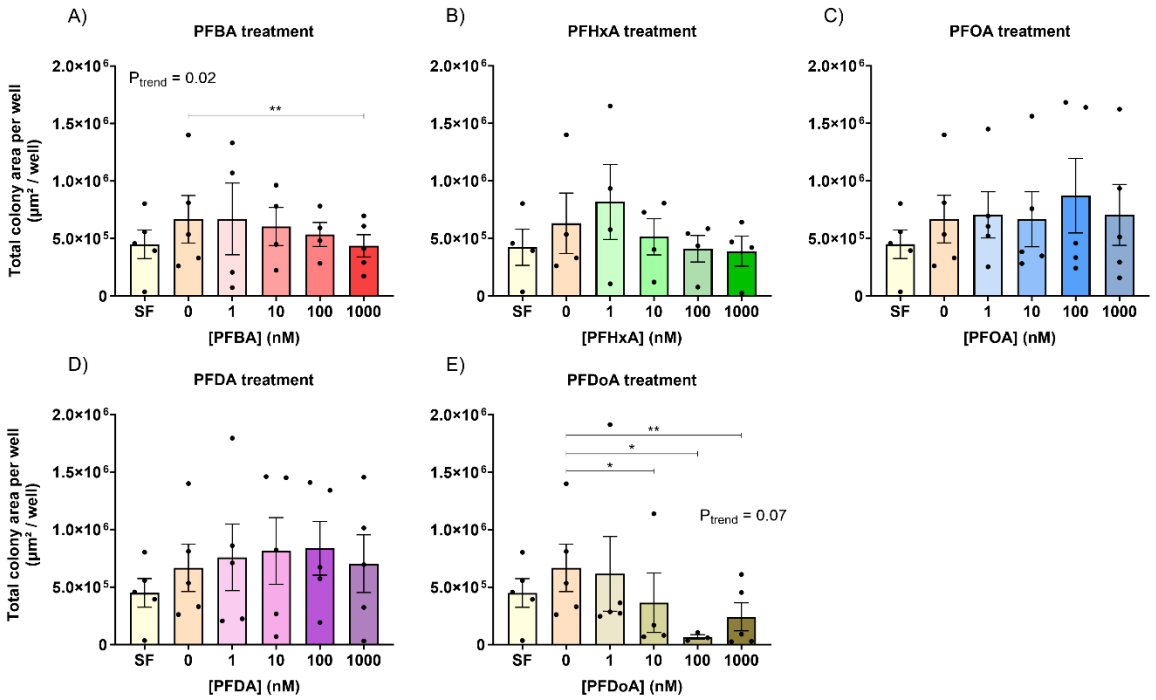


Figure 7: **Short- and long-chain PFAS concentration-response effect on Hs578T total colony area per well**. Total colony area was measured in each well after 48 hours of treatment of varying concentrations of A) PFBA, B) PFHxA, C) PFOA, D) PFDA, and E) PFDoA. 5 biological replicates were run in total for most treatment groups. Significant decreases in total colony area were seen in 1000 nM PFBA, 10 nM PFDoA, 100 nM PFDoA, and 1000 nM PFDoA. Decreasing trends were seen with increasing PFBA treatment and PFDoA treatment. Figure depicts mean ± SEM. *p ≤ 0.05, **p ≤ 0.01.

Alkyl chain length effects on invasive protrusion formation in Hs578T cells

When comparing the effects of alkyl length on the mean number of protrusions per cell, no significant effects were seen within any of the four concentrations tested (Figure 8). However, 1 nM PFAS treatment (Figure 8A) induced positive trends in the mean number of protrusions per cell that neared significance ($p = 0.06$). Upon 10 nM PFAS treatment (Figure 8B), this trend reversed ($p = 0.06$). No trends were observed in the 100 nM and 1000 nM concentrations. When comparing the effects of alkyl length on the mean longest protrusion length per cell, no significant effects were seen within any of the four concentrations tested (Figure 9).

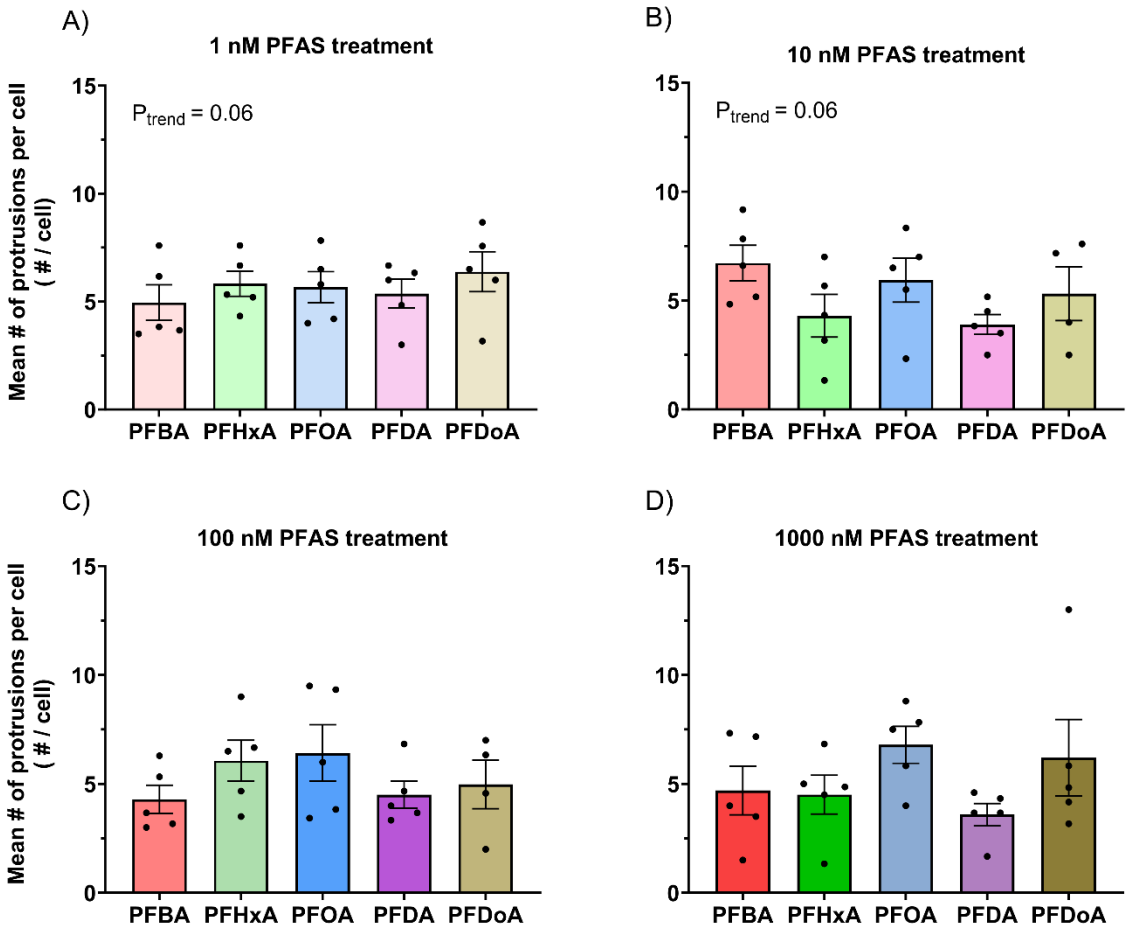


Figure 8: Alkyl chain length effect on Hs578T mean number of protrusions per cell. Cell protrusion counts were measured after 48 hours of treatment of five PFAS of increasing alkyl chain length at A) 1nM, B) 10 nM, C) 100 nM, and D) 1000 nM. 6 cells were measured per treatment; 5 biological replicates were run in total for most treatment groups. No significant differences between alkyl lengths were observed in any of the four concentrations tested. An increasing trend was seen with 1 nM PFAS treatment and a decreasing trend with 10 nM treatment. Figure depicts mean ± SEM.

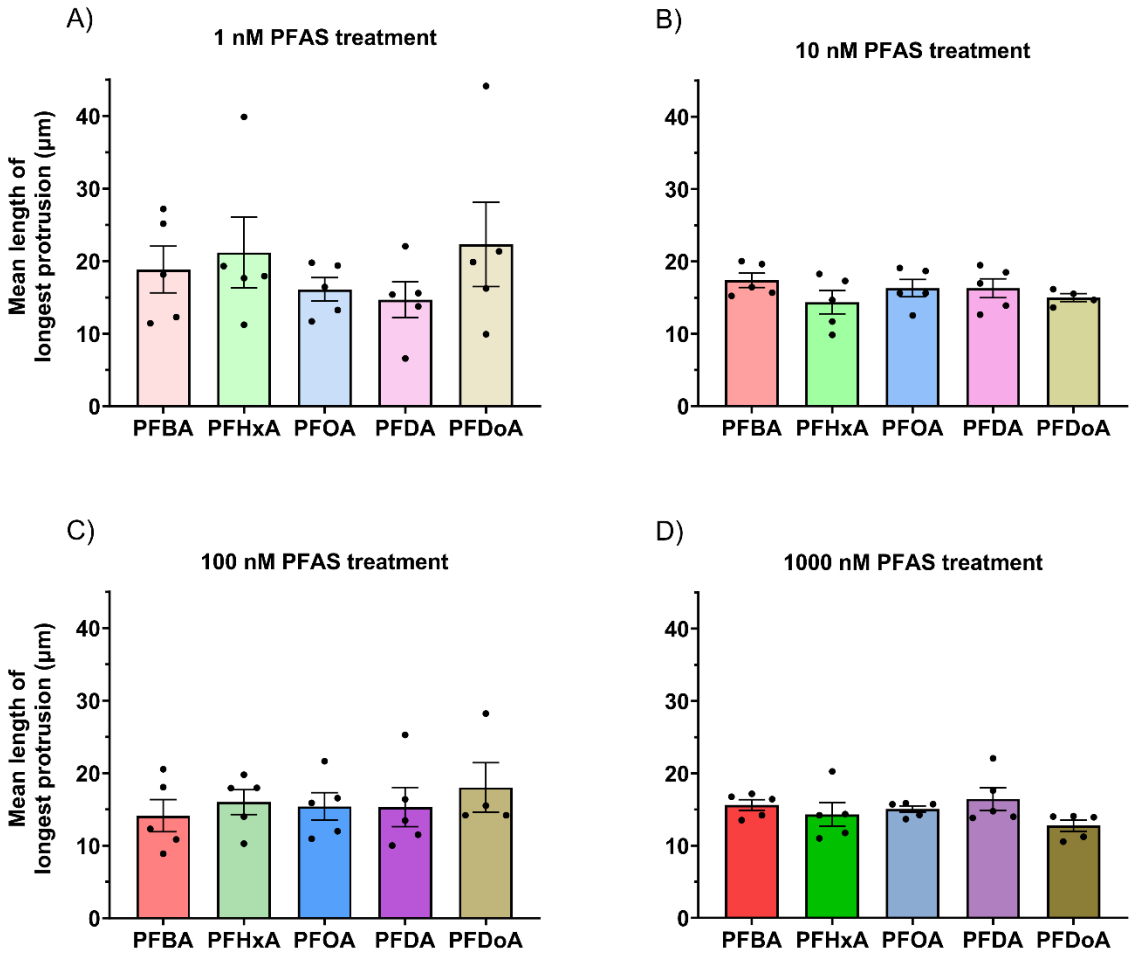


Figure 9: Alkyl chain length effects on Hs578T mean length of the longest protrusions per cell. The Longest protrusion lengths were measured after 48 hours of treatment of five PFAS of increasing alkyl chain length at A) 1nM, B) 10 nM, C) 100 nM, and D) 1000 nM. 3 - 7 cells were measured per treatment; 5 biological replicates were run in total for most treatment groups. No significant differences between alkyl lengths were observed in any of the four concentrations tested. Figure depicts mean ± SEM.

Alkyl chain length effects on total colony formation per well in Hs578T cells

When comparing the effects of alkyl length on total colony formation per well, PFDoA treated groups were the only PFAS treated groups to be significantly affected in colony formation. This effect was most pronounced in 100 nM treatment (Figure 10C), where PFDoA treatment significantly lowered total colony area per well relative to PFOA

(p = 0.03) and PFDA (p = 0.04) treated groups. Alkyl length did not affect colony formation in the rest of the concentrations tested, though the pattern of decreased colony formation with PFDoA treatment was seen in 10 nM (Figure 10B) and 1000 nM (Figure 10D) treatments.

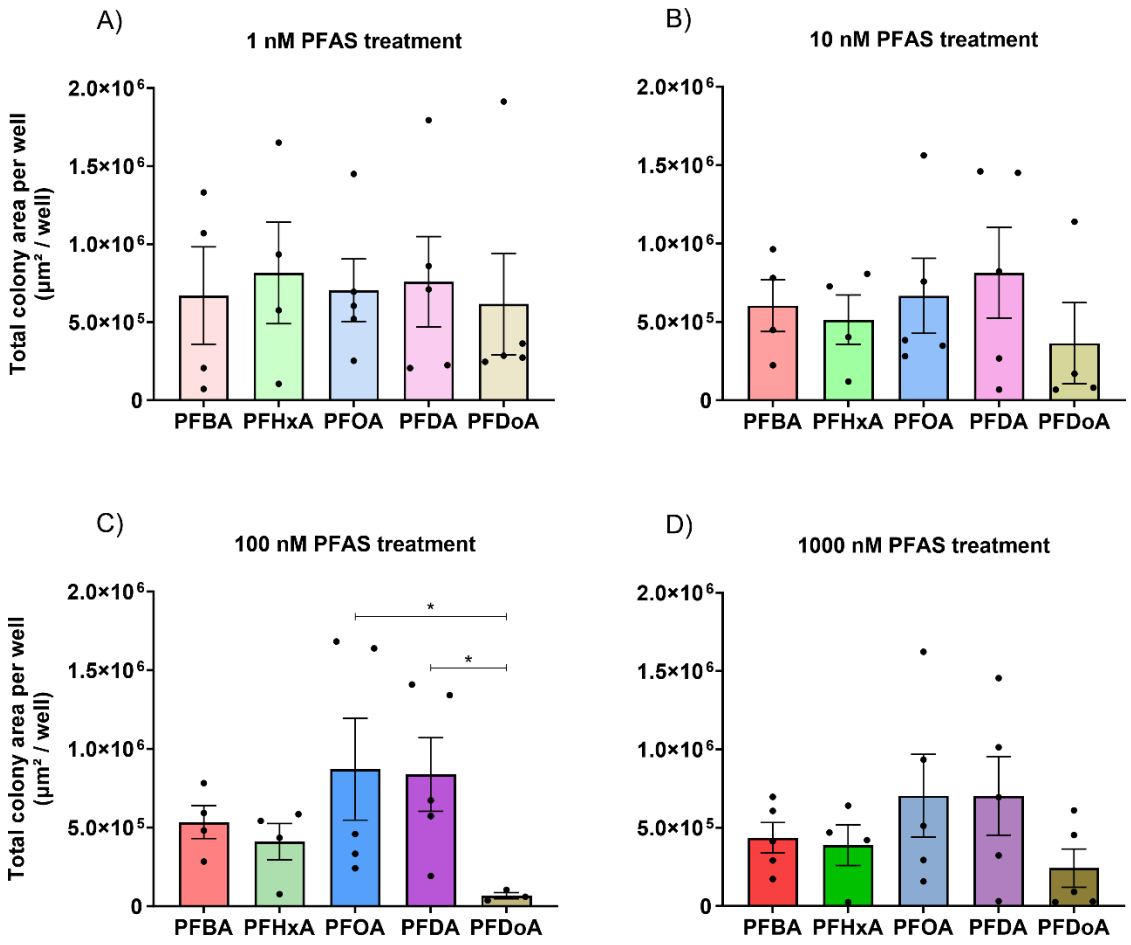


Figure 10: Alkyl chain length effects on Hs578T total colony area per well. Total colony area per well was measured after 48 hours of treatment of five PFAS of increasing alkyl chain length at A) 1nM, B) 10 nM, C) 100 nM, and D) 1000 nM. 5 biological replicates were run in total for most treatment groups. Significant decreases in colony formation were seen with 100 nM PFDoA treatment when compared to PFOA and PFDA. Significant trends were not observed. Figure depicts mean ± SEM.

Concentration effects on mean live and dead cell number per well

The concentrations of 1 nM and 10 nM were of interest for 2D cell proliferation since 2.5D findings suggested increasing alkyl length at these concentrations promoted near-significant trends in mean number of protrusions per cell (Figure 8A and 8B). These concentrations are also the most relevant to the human exposure experience, with human serum PFAS levels falling between 0 – 10 nM. No significant effects of 1 nM and 10 nM PFAS on the mean viable cell number (Figure 11) or mean non-viable cell number (Figure 12) per well were observed relative to the 5% FBS control. Batch effects are observed to highly increase variance among the three biological replicates, with replicate one consistently yielding lower viable cell number values and replicate three higher values across treatments. Additionally, 10 nM PFAS treatments are observed to consistently decrease the mean viable cell number per well relative to 1 nM treatment, though this difference was not significant.

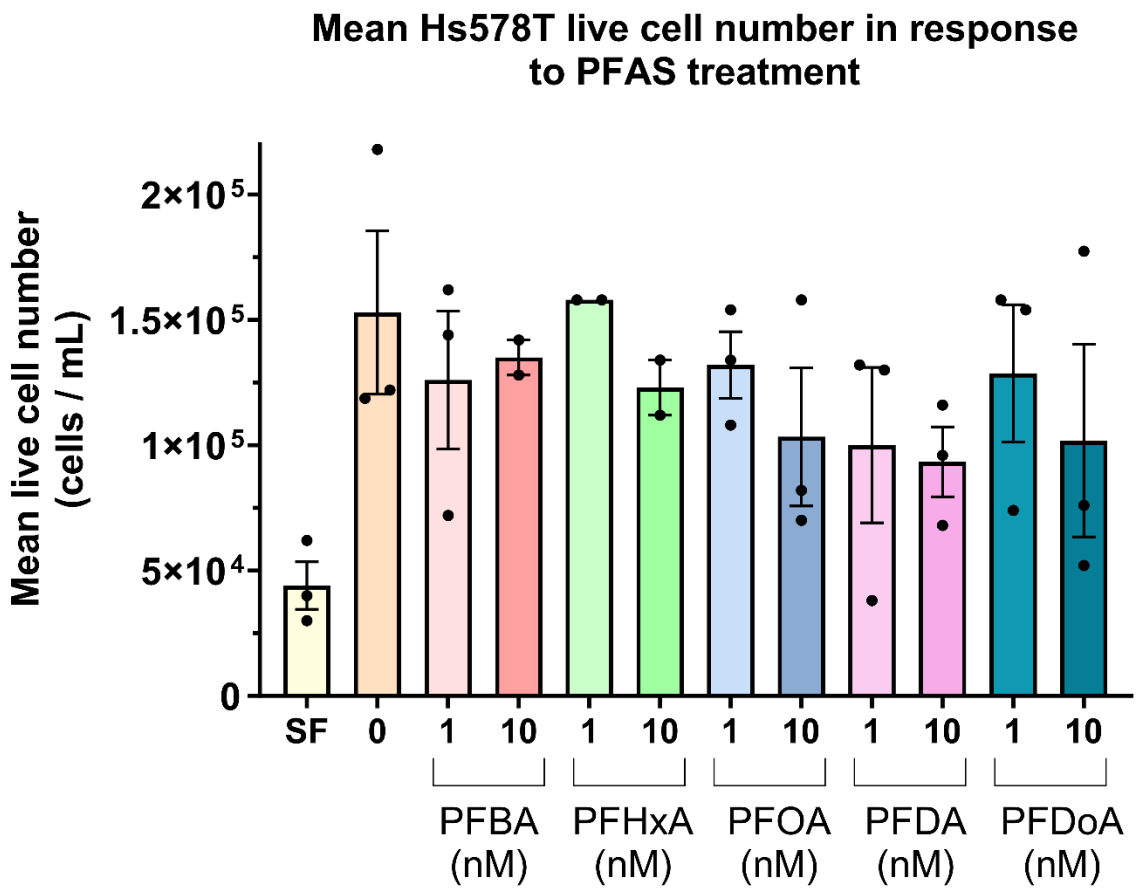


Figure 11: **Short- and long-chain PFAS treatment on Hs578T mean viable cell number per well**. Mean live cell number per well were measured after 48 hours of PFAS treatment at 1 nM and 10 nM with Trypan Blue. These concentrations did not significantly affect mean live cell number. Two technical replicates were sampled per well; three biological replicates were run in total for most groups. Figure depicts mean ± SEM.

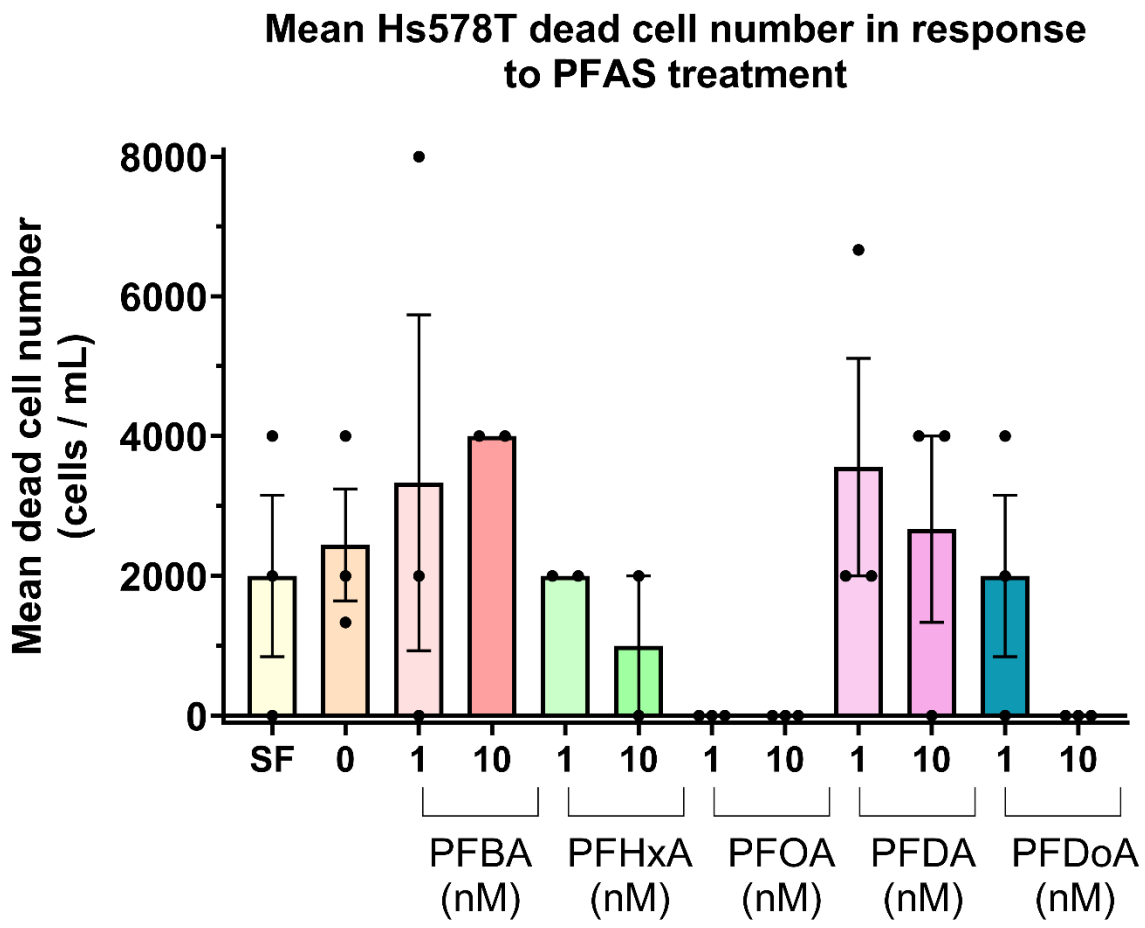


Figure 12: **Short- and long-chain PFAS treatment on Hs578T mean non-viable cell number per well**. Mean dead cell number per well were measured after 48 hours of PFAS treatment at 1 nM and 10 nM with Trypan Blue. These concentrations did not significantly affect mean dead cell number. Two technical replicates were sampled per well; three biological replicates were run in total for most groups. Figure depicts mean ± SEM.

Alkyl chain length effects on mean live cell number per well

No significant effects of increasing alkyl chain length on the mean live cell number per well were observed in either 1 nM or 10 nM treated PFAS groups (Figure 13). Batch effects are observed to highly increase variance among the three biological replicates as previously mentioned.

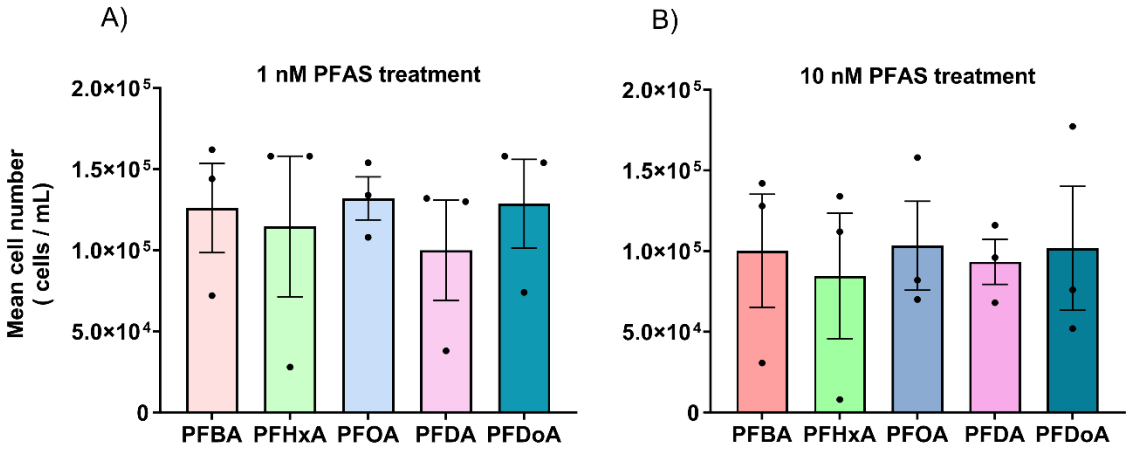


Figure 13: Alkyl chain effects on mean live cell number per well. Mean live cell number per well were measured after 48 hours of treatment of five PFAS of increasing alkyl chain length at A) 1nM and B) 10 nM PFAS with Trypan Blue. Mean live cell number was not significantly affected by alkyl chain length at either 1 nM or 10 nM PFAS treatment. Significant trends were not observed.

Discussion:

PFAS accumulation in human food and water resources is of growing concern as the production and use of these chemicals increases worldwide. Studies on the health effects of short-chain alternatives are lacking but increasingly being generated as pressure to produce data increases. Data gaps on the cancer progressive effects of the long-chain PFAS in our study are of pressing concern given their continued presence in human serum and the current findings implicating the well-characterized, structurally similar PFOA to kidney, testicular, and liver cancers[16, 37.] Additionally, IARC classified PFOA as a Group 1 carcinogen to humans in 2023[67], which stimulates concern for structurally similar PFAS. Researchers are attempting to remedy these data gaps by using GenRA methodology. Current GenRA focuses on cellular and organismal toxicities that are separate from cancer progression endpoints, which we attempted to compare in this study between PFAS of varying sizes. The association between PFAS and breast cancer remains to be debated[58, 61, 65]. The increasing evidence suggests breast cancer progression is driven by PFAS in receptor-positive[33] and possibly -negative[50] breast cancer types. Although, research and evidence for the latter is sparse[14], increased TNBC incidence rates in Black women of post-menopausal age[19] who may display higher serum levels of long-chain PFAS[12, 34, 36] support the possibility of PFAS environmental injustice. Thus, continued efforts must be made towards elucidating the PFAS – TNBC relationship.

Cell proliferation migration, and invasion are three drivers of malignant cancer progression that were investigated in our study. We found that short- and long-chain PFAS treatments across environmentally relevant concentrations were not sufficient to significantly induce a more aggressive cell phenotype using the human TNBC cell line

Hs578T in 2D or 2.5D cultures. In contrast, PFAS seem to prevent progression in some cases.

The five PFAS assessed in Hs578T significantly reduced or had no effect on the mean number of protrusions per cell. For example, high PFBA concentrations (100 nM and 1000 nM) significantly decreased the mean number of protrusions per cell reflected by a concentration-dependent decrease in protrusion counts. PFDA decreased protrusion counts across all concentrations tested, and PFDoA decreased protrusion counts at 10 nM and 100 nM concentrations. No literature has yet extracted protrusion count data from PFAS-treated human TNBC cell lines, but Zhang et al., 2014[69] demonstrated significant increases in TNBC invasion following PFOA treatment in the TNBC cell line MDA-MB-231. In contrast to our null PFOA protrusion results, the researchers showed that 5 nM, 10 nM, and 50 nM concentrations significantly increased transwell invasion after 72 hours of treatment, supported by molecular evidence.

The five PFAS generally had no effect on the mean length of the longest protrusion per cell. PFDoA was the only treatment which resulted in a concentration-dependent decrease and in which 100 nM PFDoA significantly decreased the longest protrusion length. While no literature has yet extracted cell protrusion length data from PFAS-treated human TNBC cell lines, Wang et al., 2024[63] employed similar 3D culture methods to assess cell morphology following PFBA and PFOA treatment. The researchers treated MDA-MB-231 cells with 100 nM – 1uM PFBA or PFOA for 120 hours and found 1 μM PFOA treatment to increase cell protrusion length and fissure. Protrusion lengthening and fissure are indicative of a cell's ability to detach from the basement membrane and

migrate or invade surrounding tissues. These parameters were assessed with scanning electron microscopy but were not quantified in the study.

The five PFAS assessed significantly reduced or had no effect on total colony area per well. We found that 1000 nM PFBA and 10 - 1000 nM PFDoA significantly reduced total colony area per well. Additionally, PFBA and PFDoA displayed concentration-dependent decreases in total colony area per well. PFDoA treatment reduced colony area to the lowest levels seen across treatments, possibly suggesting a cytotoxic effect in 2.5D in these cells. Currently, no literature has assessed PFAS effects on human TNBC colony formation. However, Wang et al., 2024[63] tested the effects of 100 nM – 10 μM PFBA or PFOA on MDA-MB-231 cell deformation, a well-known indicator of invasion, in 3D. After 120 hours of treatment, 1 μM PFOA significantly increased cell deformation rates. The research team also assessed cell migration using transwell inserts over the same time length, finding 1 μM of both PFAS to significantly increase the percentage of migrated cells relative to the control. In the study, the effects of migration by PFOA were greater than those of PFBA, and only PFOA-induced migration was supported by molecular evidence. Furthermore, Zhang et al., 2014[69] tested the effects of 100 μM PFOA on MDA-MB-231 wound healing migration. After 60 – 72 hours, PFOA induced significantly higher wound closure and thus migratory capability relative to the control.

Cell proliferation was then investigated to understand if PFAS promoted cell growth. This was completed by Trypan Blue staining and subsequent cell counting of both viable and non-viable cells. We found no significant effects of PFAS treatment at 1 nM or 10 nM on TNBC cell proliferation or cell death. Instead, viable cell decreases can be seen for all PFAS treated groups relative to the 5% FBS control in a concentration-dependent

fashion, though not significantly. This is unlikely to be caused by PFAS toxicity given that the cell death data are similar across treatments and relatively low compared to viable cell numbers. Strikingly, the negative and positive controls were not significantly different when analyzed among all the data via One-Way ANOVA with Tukey's post-hoc test. However, when compared via unpaired T-test, the controls were significantly different ($p = 0.004$). This highlights that the current results exhibit enough variance to mask true effects of treatment. This variance is caused by batch effects, as biological replicates one and three consistently yield lower and higher values, respectively, regardless of treatments. Current findings must be disentangled using more biological replicates and by removing batch effects. Batch effects can be removed by normalization of PFAS treated groups to the 5% FBS control or by using software to analyze the data accounting for repeated measures within biological replicates, as was completed for the 2.5D assay data (see Methods → Statistical Analysis). Originally, batch effects were also observed in the 2.5D data when using three biological replicates, thus two more replicates were supplied to better understand the results. The two additional biological replicates changed the understanding of the data significantly, and it may be the same case with the cell proliferation data. Additionally, our proliferation assay can be paired with more evidence, such as flow cytometry, immunocytochemistry, and qPCR of proliferation involved genes for a more profound understanding of PFAS effects on cell proliferation. While comparing this study's proliferation data to existing PFAS – TNBC literature may be premature given the large variance exhibited, our proliferation data currently agrees with the literature. Pierozan et al., 2022[45] tested the concentration-dependent responses of PFBA and PFHxA treated MCF10A cells (a receptor-negative breast epithelial cell line) on cell

proliferation using concentrations of 500 pM – 500 μM. After 72 hours, the researchers then assessed cell number and MTT formazan production to determine the proliferative effects of the two short-chain PFAS, finding null results at all concentrations. Similarly, Zhang et al., 2014[69] tested the effects of 0 – 150 nM PFOA on MTT formazan production of the TNBC cell line MDA-MB-231 after 72 hours, finding no effects by PFOA. Wang et al., 2024[63] tested the effects of PFBA and PFOA on Cell Counting Kit-8 formazan production of MDA-MB-231 using concentrations of 100 pM – 1 mM. After 24 - 120 hours, the researchers found that PFBA and PFOA did not affect formazan production at the concentrations and 48-hour time point we used in our study. Finally, Sakai et al., 2022[50] tested the effects of PFOA treated MDA-MB-231 cells using concentrations of 1 μM – 1 mM. After 48 hours, the researchers assessed MTS formazan production, finding that PFOA did not affect cell proliferation once more. While this last example uses concentrations two orders of magnitude higher than our proliferation assay, the four examples together suggest PFAS do not promote receptor-negative breast cell proliferative phenotypes, agreeing with our results. It is important to note, however, that MTT and MTS assays should be carefully interpreted when assessing proliferation. These two assays utilize mitochondrial reduction of MTT into formazan. PFAS may interfere with normal mitochondrial function and affect the results, thus separate proliferation assays are preferred. The latter three studies are the only ones we are aware of testing PFAS on TNBC proliferation, so our PFDA and PFDoA findings cannot be compared to existing literature.

It must be highlighted that the methods of the studies aforementioned differ greatly from ours in cell line, treatment time length, 2.5D model, and data extraction, possibly

leading to deviations from published literature. Interestingly, in our study the significant decreasing effects of PFBA and PFOA treatment are reflected in two of our parameters: the mean number of protrusions per cell and total colony formation per well. This suggests that the colony formation assay is more of an invasion assay as it is frequently described to be[10, 17, 49], rather than a migration assay which it is less associated with. It also suggests invasion is indeed hindered by these PFAS. More established migration assays need to be implemented to elucidate the effects of our treatments on TNBC migration.

When viewing the data through a GenRA approach, there were no significant effects of alkyl chain length on mean number of protrusions- or on the mean length of the longest protrusion per cell. While a positive trend in the former parameter was seen with increasing alkyl length 1 nM PFAS, the trend reversed at 10 nM PFAS, highlighting inconsistency between treatment concentrations and undermining the true effects of alkyl length on the protrusion count parameter. Alternatively, these results can be interpreted as long-chain PFAS promoting increases in mean number of protrusions per cell at low concentrations and decreases at higher concentrations as a result of toxicity. Further validation methods must be employed to determine if this is true. Colony formation seemed to be the parameter most affected by alkyl length. At 100 nM PFAS treatment, PFDoA significantly decreased total colony area per well relative to PFOA and PFDA. This pattern was also observed in 10 nm and 1000 nM PFAS treatment but was not significant. These results suggest that a combination of concentration and alkyl length may promote decreased colony formation in these cells, possibly due to cytotoxicity in the 2.5D environment. While not significant, the long-chain PFOA and PFDA seem to increase total colony formation per well in 10 nM – 1000 nM treated groups relative to

PFBA and PFHxA, displaying non-significant increasing trends. However, it is difficult to state with confidence that this is the case given the variance. When assessing cell proliferation, no effects of alkyl length on live or dead cell number were observed.

Future work

Our methods were not without limitations. For example, a downside of the 2.5D assay is that the cells can grow through the Z plane in addition to the X and Y planes, likely under sampling the protrusion counts per cell. However, this is a systematic challenge present in all treatment groups that did not affect the ability of the researchers to capture the significant differences between the controls, which eases some of this concern. In future studies, protrusion extraction can be refined using more sensitive methods such as by using cytoskeleton dyes to quantify migration and invasion by assessing effects of PFAS on actin filament formation[24]. Utilizing scanning electron microscopy has shown to capture protrusion extension and fissure development in PFOA treated MDA-MB-231 cells[63], which may also be an option. Cell protrusion formation may also be cell density dependent, where higher densities promote higher numbers of protrusions per cell due to intercell communication and close proximity. This has yet to be tested but was visually observed to occur in the 2.5D assay and is worth exploring. Additionally, the 2.5D assay can be refined by the extraction of cell proliferation data from this more biologically relevant model[10, 25, 26]. During our study, we attempted to gather cell proliferation data from the 2.5D assay using a CyQuant nucleic acid binding fluorescent dye (Cat. C7026, Thermo Fisher Scientific; Waltham, MA) following whole-cell and colony extraction from the 2.5D system. However, technical challenges in extracting all cells

hindered these efforts. In future studies, methods described in the literature to work in 3D systems can be employed such as EdU cell proliferation assays or DAPI staining. Molecular evidence often complements the phenotypic data. RNA extraction from 2.5D systems is possible, however, we experienced technical challenges in extracting good quality RNA from the 2.5D assay as confirmed by fragment analyzer analysis. This issue can be remedied with further optimizations. In the meantime, cells have been seeded and treated with 1 nM and 10 nM PFAS in the 2D environment absent of Matrigel and good quality RNA has been extracted. Thus, PCR of genes involved in the proliferation, migration, invasion, and apoptosis of cells as well as those involved in canonical cancer progression signaling cascades are currently underway at the time of this writing. Mechanisms possibly involved in TNBC progression will be elucidated and compared to the literature.

Admittedly, an obstacle in our study was an inter-person effect in the measurement of cell protrusions in 2.5D. Due to the large number of images and time commitments, blinded images were distributed to four trained researchers for protrusion data extraction. Subsequent SAS analyses of the data accounting for blinded imager revealed significant deviations between researchers in a few treatment groups within some biological replicates. This possibly leads to higher-than-expected variance between biological replicates and may explain some of the variance in our study, thus moving forward all images will be analyzed by one individual and current findings will be re-analyzed by one individual. Automation of cell protrusion data extraction is a possibility that is being explored as well, which could circumvent human error. If we focus on the cell parameter of longest protrusion length per cell, it appears that this parameter is not a good indicator

of invasiveness in Hs578T as originally believed. This cell line develops protrusions of similar lengths in serum free conditions and FBS treated groups, which could be a consequence of the highly invasive nature of this stellate breast cancer type. It was also visually apparent under light microscopy that serum starved cells plated in 2D exhibit thinner cell bodies and extended protrusions, likely a sign of poor health. Thus, it can be hypothesized that starvation stress induces cell deformation that could be mistaken for invasive protrusion formation in 2.5D. A better negative control that inhibits invasion can be used moving forward. Alternatively, the longest protrusion length parameter can be replaced with more detailed invasion parameters such as immunofluorescence of cytoskeleton proteins. On the other hand, our null results from this parameter can also be explained by our methods, specifically our technical replicate sampling scheme. As previously mentioned, six cells per well per biological replicate were selected for protrusion analysis. However, if a cell had zero protrusions it could not be incorporated into the protrusion length parameter, leading to a minimum of three cells analyzed in some treatments. This is an insufficient sample size given the heterogenous morphology of this cell line. Future work will redefine the sampling scheme to prevent under sampling. Of course, it cannot be forgotten that this work focuses on acute exposure in one cell type. True human exposure occurs at timelines from months to years, with inter-cell communication. PFAS are known to be immunotoxic and the immune system is heavily involved in tumor progression, thus the results of this study must be carefully interpreted knowing this. Future work can improve upon the methods used in this study such as by treating cells chronically and by the involvement of coculture for a better understanding of PFAS induced TNBC progression.

Conclusions

To our knowledge, this is the first study to use the 2.5D model to assess PFAS treated triple negative breast cancer cell progression by the quantification and analysis of individual cell and total colony parameters. PFAS treatment on breast cancers in 2.5D and 3D environments, which are more resemblant of the human biological experience, are severely lacking. Furthermore, Generalized Read-Across with cancer progression endpoints such as those involved in this study have yet to be explored in depth. The strength of read-across comes from the increasing number of studies assessing the same endpoints following similar treatments, which we aimed to contribute to in this study. Given that the TNBC subtype is a heterogenous disease in itself, 2.5D and 3D models must be increasingly employed using various triple negative cell lines to elucidate their relationship with PFAS exposure.

References

1) Abunada, Z., Alazaiza, M.Y.D., Bashir, M.J.K. (2020) An Overview of Per- and Polyfluoroalkyl Substances (PFAS) in the Environment: Source, Fate, Risk and Regulations. *Water*, *12*, 3590. https://doi.org/10.3390/w12123590
2) Barbo, N., Stoiber, T., Naidenko, O.V., Andrews, D.Q. (2023). Locally caught freshwater fish across the United States are likely a significant source of exposure to PFOS and other perfluorinated compounds**.** *Environmental Research, 220*, 115165.
3) Behr, A., Lichtenstein, D., Braeuning, A., Lampen, A., & Buhrke, T. (2018). Perfluoroalkylated substances (PFAS) affect neither estrogen and androgen receptor activity nor steroidogenesis in human cells in vitro. *Toxicology Letters, 291*, 51–60. https://doi.org/10.1016/j.toxlet.2018.03.029
4) Berens, E. B., Holy, J. M., Riegel, A. T., & Wellstein, A. (2015). A cancer cell spheroid assay to assess invasion in a 3D setting. *Journal of Visualized Experiments, 105*. https://doi.org/10.3791/53409
5) Biomonitoring Data Tables for Environmental Chemicals. (2024). CDC. https://www.cdc.gov/exposurereport/data_tables.html?NER_SectionItem=FDA
6) Boisvert, G., Sonne, C., Rigét, F. F., Dietz, R., & Letcher, R. J. (2019). Bioaccumulation and biomagnification of perfluoroalkyl acids and precursors in East Greenland polar bears and their ringed seal prey. *Environmental Pollution, 252(B)*, 1335–1343. https://doi.org/10.1016/j.envpol.2019.06.035
7) Bonefeld-Jorgensen, E. C., Long, M., Bossi, R., Ayotte, P., Asmund, G., Krüger, T., Ghisari, M., Mulvad, G., Kern, P., Nzulumiki, P., & Dewailly, E. (2011). Perfluorinated compounds are related to breast cancer risk in greenlandic inuit: A case control study. *Environmental Health, 10(1)*. https://doi.org/10.1186/1476-069x-10-88
8) Boone, J.S., Vigo, C., Boone, T., Byrne, C., Ferrario, J., Benson, R., Donohue, J., Simmons, J.E., Kolpin, J., Furlong, E.T., Glassmeyer, S.T. (2019). Per- and polyfluoroalkyl substances in source and treated drinking waters of the United States. *Science Of The Total Environment*, *653*, 359-369. https://doi.org/10.1016/j.scitotenv.2018.10.245
9) McDowell, S. (2022). Breast cancer death rates are highest for Black Women—Again. Breast Cancer Facts & Figures, 2022-2024. American Cancer Society. https://www.cancer.org/research/acs-research-news/breast-cancer-death-rates-are-highest-for-black-women-again.html#
10) Caiazza, F., McGowan, P. M., Mullooly, M., Murray, A., Synnott, N., O'Donovan, N., Flanagan, L., Tape, C. J., Murphy, G., Crown, J., & Duffy, M. J. (2015). Targeting ADAM-17 with an inhibitory monoclonal antibody has antitumour effects in triple-negative breast cancer cells. *British Journal of Cancer, 112(12),* 1895–1903. https://doi.org/10.1038/bjc.2015.163
11) Calafat, A. M., Kato, K., Hubbard, K., Jia, T., Botelho, J. C., & Wong, L. (2019). Legacy and alternative per- and polyfluoroalkyl substances in the U.S. general population: Paired serum-urine

data from the 2013–2014 National Health and Nutrition Examination Survey. *Environment International*, *131*, 105048. https://doi.org/10.1016/j.envint.2019.105048

12) Calafat, A. M., Wong, L., Kuklenyik, Z., Reidy, J. A., & Needham, L. L. (2007). Polyfluoroalkyl Chemicals in the U.S. Population: Data from the National Health and Nutrition Examination Survey (NHANES) 2003–2004 and Comparisons with NHANES 1999–2000. *Environmental Health Perspectives, 115(11),* 1596–1602. https://doi.org/10.1289/ehp.10598
13) California Environmental Contaminant Biomonitoring Program. (2024). Biomonitoring California priority chemicals. https://biomonitoring.ca.gov/sites/default/files/downloads/PriorityChemicalsList_March2024.pdf
14) Chang, V. C., Rhee, J., Berndt, S. I., Moore, S. C., Freedman, N. D., Jones, R. R., Silverman, D. T., Gierach, G. L., Hofmann, J. N., & Purdue, M. P. (2023). Serum perfluorooctane sulfonate and perfluorooctanoate and risk of postmenopausal breast cancer according to hormone receptor status: An analysis in the Prostate, Lung, Colorectal and Ovarian Cancer Screening Trial. *International Journal of Cancer, 153(4),* 775–782. https://doi.org/10.1002/ijc.34487
15) Chen, J., Li, N., Liu, B., Ling, J., Yang, W., Pang, X., & Li, T. (2020). Pracinostat (SB939), a histone deacetylase inhibitor, suppresses breast cancer metastasis and growth by inactivating the IL-6/STAT3 signalling pathways*. Life Sciences, 248*, 117469. https://doi.org/10.1016/j.lfs.2020.117469
16) C8 Science Panel website. (2020). http://www.c8sciencepanel.org/
17) De, P., Sun, Y., Carlson, J. H., Friedman, L. S., Leyland-Jones, B. R., & Dey, N. (2014). Doubling Down on the PI3K-AKT-mTOR Pathway Enhances the Antitumor Efficacy of PARP Inhibitor in Triple Negative Breast Cancer Model beyond BRCA-ness. *Neoplasia, 16(1),* 43-W19. https://doi.org/10.1593/neo.131694
18) De Silva, A.O., Armitage, J.M., Bruton, T.A., Dassuncao, C., Heiger-Bernays, W., Hu, X.C., Kärrman, A., Kelly, B., Ng, C., Robuck, A., Sun, M., Webster, T.F. and Sunderland, E.M. (2020). PFAS Exposure Pathways for Humans and Wildlife: A Synthesis of Current Knowledge and Key Gaps in Understanding. *Environmental Toxicology and Chemistry*, *40*, 631-657. https://doi.org/10.1002/etc.4935
19) Du, X.L., Li, Z. (2023). Incidence trends in triple-negative breast cancer among women in the United States from 2010 to 2019 by race/ethnicity, age and tumor stage. *American Journal of Cancer Research, 13(2),* 678-691.
20) Duval, K., Grover, H., Han, L., Mou, Y., Pegoraro, A. F., Fredberg, J., & Chen, Z. (2017). Modeling Physiological Events in 2D vs. 3D Cell Culture. *Physiology, 32(4),* 266–277. https://doi.org/10.1152/physiol.00036.2016
21) EPA launches stewardship program to reduce PFAS in the marketplace. (2024). US EPA. https://www.epa.gov/chemicals-under-tsca/epa-launches-stewardship-program-reduce-pfas-marketplace

22) Generalized Read-Across (GENRA). (2023). US EPA. https://www.epa.gov/comptox-tools/generalized-read-across-genra
23) GUIDELINES FOR USE. (2013). Corning Matrigel Basement Membrane Matrix Growth Factor Reduced, 10 mL Vial [Guidelines]. Corning Incorporated. https://www.corning.com/catalog/cls/documents/protocols/SPC-354230.pdf
24) Hoffmeyer, M. R., Wall, K. M., & Dharmawardhane, S. F. (2005). In vitro analysis of the invasive phenotype of SUM 149, an inflammatory breast cancer cell line. *Cancer Cell International, 5(1),* 11. https://doi.org/10.1186/1475-2867-5-11
25) Jabbari, K., Cheng, Q., Winkelmaier, G., Furuta, S., & Parvin, B. (2022). CD36+ fibroblasts secrete protein ligands that Growth-Suppress Triple-Negative breast cancer cells while elevating adipogenic markers for a model of Cancer-Associated fibroblast. *International Journal of Molecular Sciences, 23(21),* 12744. https://doi.org/10.3390/ijms232112744
26) Jabbari, K., Winkelmaier, G., Andersen, C., Yaswen, P., Quilici, D., Furuta, S., Cheng, Q., & Parvin, B. (2021). Protein ligands in the secretome of CD36+ fibroblasts induce growth suppression in a subset of breast cancer cell lines. *Cancers, 13(18),* 4521. https://doi.org/10.3390/cancers13184521
27) Kenny, P. A., Lee, G. Y., Myers, C. A., Neve, R. M., Semeiks, J. R., Spellman, P. T., Lorenz, K., Lee, E. H., Barcellos-Hoff, M. H., Petersen, O. W., Gray, J. W., & Bissell, M. J. (2007). The morphologies of breast cancer cell lines in three-dimensional assays correlate with their profiles of gene expression. *Molecular Oncology, 1(1),* 84–96. https://doi.org/10.1016/j.molonc.2007.02.004
28) Kim, K., Bennett, D. H., Calafat, A. M., Hertz-Picciotto, I., & Shin, H. (2020). Temporal trends and determinants of serum concentrations of per- and polyfluoroalkyl substances among Northern California mothers with a young child, 2009–2016. *Environmental Research, 186*, 109491. https://doi.org/10.1016/j.envres.2020.109491
29) Kjeldsen, L. S., & Bonefeld-Jørgensen, E. C. (2013). Perfluorinated compounds affect the function of sex hormone receptors. *Environmental Science and Pollution Research International, 20(11),* 8031–8044. https://doi.org/10.1007/s11356-013-1753-3
30) Lee, G. Y., Kenny, P. A., Lee, E. H., & Bissell, M. J. (2007). Three-dimensional culture models of normal and malignant breast epithelial cells. Nature Methods, 4(4), 359–365. https://doi.org/10.1038/nmeth1015
31) Li, J., Zhang, T., Yang, F., He, Y., Dai, F., Gao, D., Chen, Y., Liu, M., & Yi, Z. (2015). Inhibition of breast cancer progression by a novel histone deacetylase inhibitor, LW479, by down-regulating EGFR expression. *British Journal of Pharmacology, 172(15),* 3817–3830. https://doi.org/10.1111/bph.13165
32) Liu, M., Nordstrom, M., Forand, S., Lewis-Michl, E., Wattigney, W. A., Kannan, K., Wang, W., Irvin-Barnwell, E., & Hwang, S. (2022). Assessing exposures to per- and polyfluoroalkyl

substances in two populations of Great Lakes Basin fish consumers in Western New York State. *International Journal of Hygiene and Environmental Health, 240*, 113902. https://doi.org/10.1016/j.ijheh.2021.113902

33) Maras, M., Vanparys, C., Muylle, F., Robbens, J., Berger, U., Barber, J. L., Blust, R., & De Coen, W. (2005). Estrogen-Like properties of fluorotelomer alcohols as revealed by MCF-7 breast cancer cell proliferation. *Environmental Health Perspectives*, *114(1),* 100–105. https://doi.org/10.1289/ehp.8149
34) Nelson, J. W., Scammell, M. K., Hatch, E. E., & Webster, T. F. (2012). Social disparities in exposures to bisphenol A and polyfluoroalkyl chemicals: a cross-sectional study within NHANES 2003-2006. *Environmental Health, 11(1).* https://doi.org/10.1186/1476-069x-11-10
35) New Chemicals Program Review of alternatives for PFOA and related chemicals. (2024). US EPA. https://www.epa.gov/assessing-and-managing-chemicals-under-tsca/new-chemicals-program-review-alternatives-pfoa-and
36) Nguyen, V. K., Kahana, A., Heidt, J., Polemi, K., Kvasnicka, J., Jolliet, O. J., & Colacino, J. A. (2020). A comprehensive analysis of racial disparities in chemical biomarker concentrations in United States women, 1999–2014. *Environment International, 137*, 105496. https://doi.org/10.1016/j.envint.2020.105496
37) Nicole, W. (2013). PFOA and Cancer in a Highly Exposed Community: New Findings from the C8 Science Panel. *Environmental Health Perspectives, 121(11–12)*, A340. https://doi.org/10.1289/ehp.121-a340
38) Olsen, G. W., Mair, D. C., Lange, C. C., Harrington, L. M., Church, T. R., Goldberg, C. L., Herron, R. M., Hanna, H., Nobiletti, J. B., Rios, J. A., Reagen, W. K., & Ley, C. A. (2017). Per- and polyfluoroalkyl substances (PFAS) in American Red Cross adult blood donors, 2000–2015. *Environmental Research, 157*, 87–95. https://doi.org/10.1016/j.envres.2017.05.013
39) Owston, H. E., Ganguly, P., Tronci, G., Russell, S. J., Giannoudis, P. V., & Jones, E. A. (2019). Colony Formation, Migratory, and Differentiation Characteristics of Multipotential Stromal Cells (MSCs) from “Clinically Accessible” Human Periosteum Compared to Donor-Matched Bone Marrow MSCs. *Stem Cells International, 2019(1),* 1–14. https://doi.org/10.1155/2019/6074245
40) Perfluoroalkyl and polyfluoroalkyl substances (PFAS). National Institute of Environmental Health Sciences. https://www.niehs.nih.gov/health/topics/agents/pfc#:~:text=PFAS%20are%20a%20group%20of,the%20U.S.%20Environmental%20Protection%20Agency
41) Per- and polyfluoroalkyl substances (PFAS). (2024). US EPA. https://www.epa.gov/sdwa/and-polyfluoroalkyl-substances-pfas
42) PFAS Exposure Assessments Final report. (2022). ATSDR. https://doi.org/10.15620/cdc:122063
43) Pham, P. V. (2018). Medical biotechnology: Techniques and Applications. *Omics Technologies and Bio-Engineering*, 449–469. https://doi.org/10.1016/b978-0-12-804659-3.00019-1

44) Pierozan, P., Cattani, D., & Karlsson, O. (2020). Perfluorooctane sulfonate (PFOS) and perfluorooctanoic acid (PFOA) induce epigenetic alterations and promote human breast cell carcinogenesis in vitro. *Archives of Toxicology, 94(11),* 3893–3906. https://doi.org/10.1007/s00204-020-02848-6

45) Pierozan, P., Cattani, D., & Karlsson, O. (2022). Tumorigenic activity of alternative per- and polyfluoroalkyl substances (PFAS): Mechanistic in vitro studies. *Science of the Total Environment, 808*, 151945. https://doi.org/10.1016/j.scitotenv.2021.151945

46) Pierozan, P., Jerneren, F., & Karlsson, O. (2018). Perfluorooctanoic acid (PFOA) exposure promotes proliferation, migration and invasion potential in human breast epithelial cells. *Archives of Toxicology*, *92(5),* 1729–1739. https://doi.org/10.1007/s00204-018-2181-4

47) Pierozan, P., Kosnik, M., & Karlsson, O. (2023). High-content analysis shows synergistic effects of low perfluorooctanoic acid (PFOS) and perfluorooctane sulfonic acid (PFOA) mixture concentrations on human breast epithelial cell carcinogenesis. *Environment International*, *172*, 107746. https://doi.org/10.1016/j.envint.2023.107746

48) Results for Perfluoroalkyl and Polyfluoroalkyl Substances (PFASs). Biomonitoring California. https://biomonitoring.ca.gov/results/chemical/2183

49) Rao, S. S., Stoehr, J., Dokic, D., Wan, L., Decker, J. T., Konopka, K., Thomas, A. L., Wu, J., Kaklamani, V. G., Shea, L. D., & Jeruss, J. S. (2017). Synergistic effect of eribulin and CDK inhibition for the treatment of triple negative breast cancer. *Oncotarget, 8(48),* 83925–83939. https://doi.org/10.18632/oncotarget.20202

50) Sakai, G., Hirao-Suzuki, M., Koga, T., Kobayashi, T., Kamishikiryo, J., Tanaka, M., Fujii, K., Takiguchi, M., Sugihara, N., Toda, A., & Takeda, S. (2022). Perfluorooctanoic acid (PFOA) as a stimulator of estrogen receptor-negative breast cancer MDA-MB-231 cell aggressiveness: Evidence for involvement of fatty acid 2-hydroxylase (FA2H) in the stimulated cell migration. *Journal of Toxicological Sciences*, *47(4),* 159–168. https://doi.org/10.2131/jts.47.159

51) Sala-Hamrick, K. E., Tapaswi, A., Polemi, K. M., Nguyen, V. K., & Colacino, J. A. (2024). High-Throughput transcriptomics of nontumorigenic breast cells exposed to environmentally relevant chemicals. *Environmental Health Perspectives, 132(4).* https://doi.org/10.1289/ehp12886

52) Schildroth, S., Rodgers, K. M., Strynar, M., McCord, J., Poma, G., Covaci, A., & Dodson, R. E. (2022). Per-and polyfluoroalkyl substances (PFAS) and persistent chemical mixtures in dust from U.S. colleges. *Environmental Research, 206*, 112530. https://doi.org/10.1016/j.envres.2021.112530

53) Shah, I., Liu, J., Judson, R. S., Thomas, R. S., & Patlewicz, G. (2016). Systematically evaluating read-across prediction and performance using a local validity approach characterized by chemical structure and bioactivity information. *Regulatory Toxicology and Pharmacology, 79,* 12–24. https://doi.org/10.1016/j.yrtph.2016.05.008

54) Sibinski LJ: Final report of a two year oral (diet) toxicity and carcinogenicity study of fluorochemical FC-143 (perfluorooctanane ammonium carboxylate) in rats. (1987). 3M Company/RIKER Exp No 0281CR0012; 8EHQ-1087-0394. 1-4.
55) Triple-negative breast cancer- Details, diagnosis, and signs. American Cancer Society. https://www.cancer.org/cancer/types/breast-cancer/about/types-of-breast-cancer/triple-negative.html
56) Trowbridge, J., Gerona, R. R., Lin, T., Rudel, R. A., Bessonneau, V., Buren, H., & Morello-Frosch, R. (2020). Exposure to perfluoroalkyl substances in a cohort of women firefighters and office workers in San Francisco. *Environmental Science & Technology*, *54(6),* 3363–3374. https://doi.org/10.1021/acs.est.9b05490
57) Tsai, M., Chang, S., Kuo, W., Kuo, C., Li, S., Wang, M., Chang, D., Lu, Y., Huang, C., Cheng, A., Lin, C., & Chen, P. (2020). A case-control study of perfluoroalkyl substances and the risk of breast cancer in Taiwanese women. *Environment International, 142*, 105850. https://doi.org/10.1016/j.envint.2020.105850
58) U.S. Department of Health and Human Services. Agency for Toxic Substances and Disease Registry. Toxicological Profile for Perfluoroalkyls (2021). https://www.atsdr.cdc.gov/toxprofiles/tp200.pdf
59) U.S. Environmental Protection Agency. (2020a). National Coastal Condition Assessment 2015 Technical Support Document [Report]. https://www.epa.gov/system/files/documents/2022-07/NCCA%202015%20TSD%20FINAL.20210901.pdf
60) U.S. Environmental Protection Agency. (2020). National Rivers and Streams Assessment 2013–2014 Technical Support Document. https://www.epa.gov/sites/default/files/2020-12/documents/nrsa_2013-14_final_tsd_12-15-2020.pdf
61) Velarde, M. C., Chan, A. F. O., Sajo, M. E. J. V., Zakharevich, I., Melamed, J., Uy, G. L. B., Teves, J. M. Y., Corachea, A. J. M., Valparaiso, A. P., Macalindong, S. S., Cabaluna, N. D., Dofitas, R. B., Giudice, L. C., & Gerona, R. R. (2022). Elevated levels of perfluoroalkyl substances in breast cancer patients within the Greater Manila Area. *Chemosphere, 286*, 131545. https://doi.org/10.1016/j.chemosphere.2021.131545
62) Villeneuve, D. L., Blackwell, B. R., Cavallin, J. E., Collins, J., Hoang, J. X., Hofer, R. N., Houck, K. A., Jensen, K. M., Kahl, M. D., Kutsi, R. N., Opseth, A. S., Rodriguez, K. J. S., Schaupp, C., Stacy, E. H., & Ankley, G. T. (2023). Verification of in vivo estrogenic activity for four per- and polyfluoroalkyl substances (PFAS) identified as estrogen receptor agonists via new approach methodologies. *Environmental Science & Technology, 57(9),* 3794–3803. https://doi.org/10.1021/acs.est.2c09315
63) Wang, H., Zhang, H., Hu, S., Xu, T., Yang, Y., Cao, M., Wei, S., Song, Y., Han, J., & Yin, D. (2024). Insight into the differential toxicity of PFOA and PFBA based on a 3D-cultured MDA-MB-

231 cell model. *Journal of Hazardous Materials, 465*, 133499. https://doi.org/10.1016/j.jhazmat.2024.133499

64) Willis, C. M., & Klüppel, M. (2014). Chondroitin Sulfate-E is a negative regulator of a Pro-Tumorigenic WNT/Beta-Catenin-Collagen 1 axis in breast cancer cells. *PloS One, 9(8),* e103966. https://doi.org/10.1371/journal.pone.0103966

65) Yang, J., Zhang, K., Shi, J., Li, Z., Dai, H., & Yang, W. (2024). Perfluoroalkyl and polyfluoroalkyl substances and Cancer risk: results from a does-response Meta-analysis. *Journal of Environmental Health Science & Engineering*. https://doi.org/10.1007/s40201-024-00899-w

66) Young, W., Wiggins, S., Limm, W., Fisher, C.M., DeJager, L., Genualdi, S. (2022). Analysis of Per- and Poly(fluoroalkyl) Substances (PFASs) in Highly Consumed Seafood Products from U.S. Markets. *Journal of Agricultural and Food Chemistry, 70(42),* 13545-13553.

67) Zahm, S., Bonde, J. P., Chiu, W. A., Hoppin, J., Kanno, J., Abdallah, M., Blystone, C. R., Calkins, M. M., Dong, G., Dorman, D. C., Fry, R., Guo, H., Haug, L. S., Hofmann, J. N., Iwasaki, M., Machala, M., Mancini, F. R., Maria-Engler, S. S., Møller, P., . . . Schubauer-Berigan, M. K. (2024). Carcinogenicity of perfluorooctanoic acid and perfluorooctanesulfonic acid. *The Lancet Oncology, 25(1),* 16–17. https://doi.org/10.1016/s1470-2045(23)00622-8

68) Zeng, Z., Song, B., Xiao, R., Zeng, G., Gong, J., Chen, M., Xu, P., Zhang, P., Shen, M., & Yi, H. (2019). Assessing the human health risks of perfluorooctane sulfonate by in vivo and in vitro studies. *Environment International*, *126*, 598–610. https://doi.org/10.1016/j.envint.2019.03.002

69) Zhang, W., Wang, F., Xu, P., Miao, C., Zeng, X., Cui, X., Lu, C., Xie, H., Yin, H., Chen, F., Ma, J., Gao, S., & Fu, Z. (2014). Perfluorooctanoic acid stimulates breast cancer cells invasion and up-regulates matrix metalloproteinase-2/-9 expression mediated by activating NF-κB. *Toxicology Letters, 229(1),* 118–125. https://doi.org/10.1016/j.toxlet.2014.06.004